

pubs.acs.org/JPCA Article

# Chemistry of Secondary Organic Aerosol Formation from Reactions of Monoterpenes with OH Radicals in the Presence of NO<sub>x</sub>

Published as part of The Journal of Physical Chemistry virtual special issue "Advances in Atmospheric Chemical and Physical Processes".

Marla P. DeVault, Anna C. Ziola, and Paul J. Ziemann\*



Cite This: J. Phys. Chem. A 2022, 126, 7719-7736



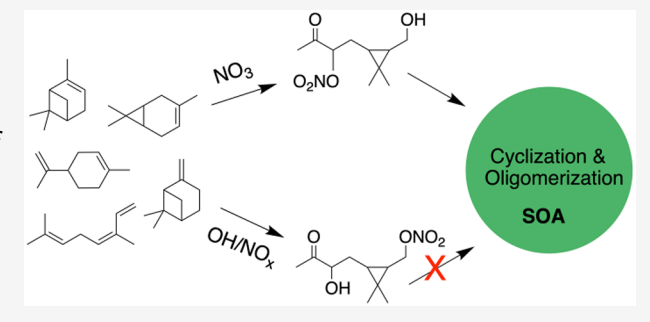
**ACCESS** 

III Metrics & More

Article Recommendations

Supporting Information

ABSTRACT: The oxidation of volatile organic compounds (VOCs), which are emitted to the atmosphere from natural and anthropogenic sources, leads to the formation of ozone and secondary organic aerosol (SOA) particles that impact air quality and climate. In the study reported here, we investigated the products of the reactions of five biogenic monoterpenes with OH radicals (an important daytime oxidant) under conditions that mimic the chemistry that occurs in polluted air, and developed mechanisms to explain their formation. Experiments were conducted in an environmental chamber, and information on the identity of gas-phase molecular products was obtained using online mass spectrometry, while liquid chromatog-



raphy and two methods of functional group analysis were used to characterize the SOA composition. The gas-phase products of the reactions were similar to those formed in our previous studies of the reactions of these monoterpenes with  $NO_3$  radicals (an important nighttime oxidant), in that they all contained various combinations of nitrate, carbonyl, hydroxyl, ester, and ether groups. But in spite of this, less SOA was formed in  $OH/NO_x$  reactions and it was composed of monomers, while SOA formed in  $NO_3$  radical reactions consisted of acetal and hemiacetal oligomers formed by particle-phase accretion reactions. In addition, it appeared that some monomers underwent particle-phase hydrolysis, whereas oligomers did not. These differences are due primarily to the arrangement of hydroxyl, carbonyl, nitrate, and ether groups in the monomers, which can in turn be explained by differences in OH and  $NO_3$  radical reaction mechanisms. The results provide insight into the impact of VOC structure on the amount and composition of SOA formed by atmospheric oxidation, which influence important aerosol properties such as volatility and hygroscopicity.

#### ■ INTRODUCTION

Large quantities of biogenic volatile organic compounds (BVOCs) are emitted to the atmosphere each year, with  $\sim$ 15% being C<sub>10</sub>H<sub>16</sub> monoterpenes that contain one or more highly reactive C=C double bonds. In the atmosphere these compounds react with OH radicals, O3, and NO3 radicals on time scales that range from a few minutes to a few hours<sup>2</sup> to form products that are usually much less volatile than the parent monoterpene and can condense to form secondary organic aerosol (SOA).<sup>3,4</sup> SOA comprises a significant fraction of the mass of atmospheric aerosol particles<sup>5,6</sup> and has important effects on visibility, human health, climate, and atmospheric chemistry. Reactions of monoterpenes with OH radicals (typically during the day) in high  $NO_x$  (NO +  $NO_2$ ) environments and reactions with NO<sub>3</sub> radicals (typically during the night) lead to the formation of organic nitrates, which can impact O<sub>3</sub> concentrations by acting as a sink for NO<sub>21</sub> and also SOA formation.<sup>8-14</sup> These reactions also add functional groups such as carbonyl, hydroxyl, carboxyl, ester, and hydroperoxide (depending on the structure of the BVOC and the oxidation conditions), most of which can participate in particle-phase accretion reactions that form high molecular weight oligomers. $^{2-4,15-17}$ 

In previous environmental chamber studies we identified and quantified gas- and particle-phase products and developed mechanisms for reactions of cyclic and acyclic monoterpenes with NO<sub>3</sub> radicals, <sup>15–17</sup> and also terminal, internal, and branched acyclic alkenes with OH/NO<sub>x</sub>. <sup>18,19</sup> All of these reactions form gas-phase products that contain various combinations of nitrate, carbonyl, and hydroxyl groups. But when products of the reactions of cyclic monoterpenes with NO<sub>3</sub> radicals that contained all three groups partitioned to particles, cyclic hemiacetals were rapidly formed by the

Received: June 30, 2022 Revised: August 24, 2022 Published: October 17, 2022





intramolecular reaction of carbonyl and hydroxyl groups, which then reacted with each other and with hydroxynitrates to form hemiacetal and acetal oligomers. Accretion reactions occurred to a much lesser extent between products of the reaction of an acyclic monoterpene with NO<sub>3</sub> radicals, <sup>17</sup> and barely at all in SOA formed from reactions of simple acyclic alkenes with OH/NO<sub>x</sub>. 18,19 This difference can be explained by the presence of a nitrate group adjacent to the carbonyl group in the ring-opened products of the reactions of cyclic monoterpenes with NO<sub>3</sub> radicals, which activates the carbonyl group toward these particle-phase reactions. 20 Other important differences were that during ring opening of cyclic monoterpenes via C-C bond cleavage the carbon backbone remained intact, whereas for the acyclic monoterpene and simple alkenes this led to more volatile fragmentation products. The NO<sub>3</sub> radical-initiated reactions also formed peroxides via ring closure, as well as carboxyl and ester groups. 15-17

In this study we investigated the gas- and particle-phase products of the reactions of four cyclic monoterpenes ( $\Delta$ -3-carene,  $\beta$ -pinene,  $\alpha$ -pinene, and limonene) and one acyclic monoterpene (ocimene) with OH/NO<sub>x</sub>, for comparison with the results of our studies of the reactions of these same compounds with NO<sub>3</sub> radicals. Mass spectrometry, gas and liquid chromatography, derivatization, UV/vis and infrared spectroscopy, and gravimetry were employed to determine SOA functional group composition, identify molecular products, and measure SOA yields. The results demonstrate the important effects of monoterpene structure and oxidation conditions on gas-phase reaction products, SOA formation and composition, and the fate of organic nitrates.

# **■ EXPERIMENTAL METHODS**

Chemicals. The following chemicals with stated/measured purities or grades and suppliers were used: (1s)-(+)-3-carene (99/100%), ocimene (90/86%), acetonitrile (HPLC grade), benzoyl peroxide (98%), and triphenylphosphine (99+%) from Sigma-Aldrich; water (HPLC grade) from Macron; ethyl acetate (HPLC grade), methanol (HPLC grade), and ammonium sulfate (99+%) from Fisher Chemical; (1S)-(-)- $\beta$ -pinene (99/89%), (1R)-(+)- $\alpha$ -pinene (99/86%), (R)-(+)-limonene (97/80%), 2-ethylhexyl nitrate (97%), bis(2ethylhexyl) sebacate (97%), tridecanoic acid (98%), and 1,2tetradecanediol (90%) from Aldrich Chemical Co.; 3hexadecanone (95%) from Alfa Aesar; NO from Matheson Tri Gas; and ultrahigh purity (UHP) N2 and He from Airgas. Methyl nitrite was synthesized as in Taylor et al.<sup>21</sup> and stored in a lecture bottle. Numerous other chemicals were used for derivatization-spectrophotometric analysis and are listed elsewhere.22-

**Environmental Chamber Experiments.** Experiments were conducted in a  $\sim$ 7 m<sup>325</sup> Teflon environmental chamber at room temperature ( $\sim$ 23 °C) and pressure ( $\sim$ 630 Torr) and 55% relative humidity (RH), as measured with a Vaisala HMP110 RH probe. The chamber was filled with clean, dry air from two AADCO pure air generators (<5 ppbv hydrocarbons and <1% RH), with water vapor added from a hot glass bulb in a flow of N<sub>2</sub>. Aqueous (NH<sub>4</sub>)<sub>2</sub>SO<sub>4</sub> seed particles were generated using a Collison atomizer and flushed into the chamber in a flow of N<sub>2</sub> to obtain a mass concentration of  $\sim$ 200  $\mu$ g m<sup>-3</sup>. Since the chamber RH was above the efflorescence RH of (NH<sub>4</sub>)<sub>2</sub>SO<sub>4</sub> of  $\sim$ 35%, <sup>26</sup> the particles remained liquid. Thermodynamic calculations indicate that

because of the evaporation of NH<sub>3</sub> these particles have pH of  $\sim$ 1, <sup>24</sup> which is comparable to values observed in the Southern Oxidants and Aerosol Study (SOAS) in the southeast United States<sup>27</sup> and in remote areas during multiple aircraft campaigns.<sup>28</sup> The monoterpene, methyl nitrite, and NO were then each added from a glass bulb (with mild heating for the monoterpene) in a flow of N<sub>2</sub> to achieve concentrations of approximately 1, 5, and 5 ppmv (1 ppmv =  $2.03 \times 10^{13}$ molecules cm<sup>-3</sup> at Boulder, CO pressure). The amount of monoterpene added was determined by using a microsyringe, while the amounts of methyl nitrite and NO were determined by filling a calibrated glass bulb on a vacuum manifold to a pressure measured using a Baratron pressure gauge. After each chemical was added, a Teflon-coated fan was turned on for 30 s to mix the chamber. Reactions were initiated by turning on 50% of the blacklights ( $J_{NO_2} = 0.19 \text{ min}^{-1}$ ) that cover two opposite walls of the chamber, forming OH radicals by photolysis of methyl nitrite according to the following reactions: 29

$$CH_3ONO + h\nu \rightarrow CH_3O \cdot + NO$$
 (1)

$$CH_3O \cdot + O_2 \rightarrow CH_2O + HO_2 \tag{2}$$

$$HO_2 + NO \rightarrow OH + NO_2$$
 (3)

The added NO guaranteed that RO2 radicals only reacted with NO, enhanced the conversion of HO2 to OH radicals, and prevented O<sub>3</sub> and NO<sub>3</sub> radical formation. The lights were turned off after ~90-240 s, when Vocus PTR-TOF measurements indicated that  $\sim$ 50% of the monoterpene had reacted. These conditions limited reactions to the formation of firstgeneration products and some second-generation products, and were chosen in order to avoid excessive chemical complexity and thus improve our chances of identifying a significant fraction of the products and determining the mechanisms by which they were formed. One  $\beta$ -pinene experiment was also conducted in dry air without seed particles to evaluate the possibility of hydrolysis of tertiary organic nitrates in the SOA, and one experiment was conducted with 2-methyl-1-tridecene to generate hydroxynitrate standards for infrared analysis.<sup>30</sup>

Gas-Phase Analysis. Gas-phase products were monitored in real time using a TOFWERK ion mobility spectrometrytime-of-flight (IMS-TOF) instrument,<sup>31</sup> with the IMS cell removed and an I- chemical ionization source replacing the electrospray ionization source normally used for solution analysis. I ions were generated by flowing N<sub>2</sub> past a CH<sub>3</sub>I permeation tube and then into an ionizing Po-210 source. The flow was then mixed with chamber air (sampled at 2 L min<sup>-1</sup> through a 0.5 m PFA tube) in an ion-molecule reactor maintained at 68 Torr, and the resulting ions were sampled into a high-resolution time-of-flight mass spectrometer (HR-TOF-MS) for mass analysis at a rate of 2 Hz. Mass spectra were generated using the Tofware analysis program in Igor Pro 7. The I<sup>-</sup> chemical ionization mass spectrometer (I-CIMS) detected all major oxygenated products, including some C<sub>10</sub> dicarbonyls, but not the monoterpene. Instead, the monoterpene concentration was monitored using a TOFWERK Vocus proton transfer reaction TOF-MS instrument.<sup>32</sup>

**Particle-Phase Analysis.** Aerosol size distributions and volume concentrations were monitored in real time using a scanning mobility particle sizer (SMPS).<sup>22</sup> When the reaction was over and the SOA mass concentration stabilized, particles

Scheme 1. Proposed Gas-Phase Mechanisms for Forming First-Generation Products from the Reactions of  $\Delta$ -3-Carene, Limonene, and Ocimene with OH Radicals in the Presence of  $NO_x^a$ 

 $^a$ The numbers in brackets correspond to the compound molecular weight/ $I^-$  adduct mass.

were collected on preweighed 0.45  $\mu$ m Millipore Fluoropore PTFE filters for 2 h at 14 L min<sup>-1</sup>. Filters were reweighed, and the SOA (without the insoluble (NH<sub>4</sub>)<sub>2</sub>SO<sub>4</sub> seed particles)

was extracted twice into 4 mL of ethyl acetate. The ethyl acetate was then evaporated in a stream of  $N_2$ , and the dried SOA was weighed. As expected, the SOA mass was  ${\sim}15{-}20\%$ 

Scheme 2. Proposed Gas-Phase Mechanism for Forming First-Generation Products from the Reaction of  $\alpha$ -Pinene with OH Radicals in the Presence of NO<sub>x</sub><sup>a</sup>

 $^a$ The numbers in brackets correspond to the compound molecular weight/ $I^-$  adduct mass.

less than the mass measured on filters, which included the unextracted  $(NH_4)_2SO_4$ . The agreement between the extracted SOA mass and the mass of SOA collected on filters indicated

an extraction efficiency of  $\sim 100\%$  and no loss of semivolatile products by evaporation, similar to results of our previous studies. The dried SOA extract was dissolved in

Scheme 3. Proposed Gas-Phase Mechanism for Forming First-Generation Products from the Reaction of  $\beta$ -Pinene with OH Radicals in the Presence of NO<sub>x</sub><sup>a</sup>

<sup>a</sup>The numbers in brackets correspond to the compound molecular weight/I<sup>-</sup> adduct mass.

acetonitrile to match the solvent used in high-performance liquid chromatography (HPLC) and stored at  $-20~^{\circ}$ C until analyzed. Analyses were conducted within a week or less, and

when replicate analyses were conducted after this time no significant differences were observed. Although extraction could lead to the dissociation of weakly bound oligomers formed through reversible reactions, such as hemiacetals, these types of oligomers were observed in our previous studies of SOA formed from reactions of monoterpenes with NO<sub>3</sub> radicals that employed the same methods. Sample processing did not lead to the formation of oligomers, since none were detected in subsequent analyses. Filters were weighed to  $\pm 0.5 \mu g$  using a Mettler Toledo XS3DU microbalance, and extracts were weighed to ±0.05 mg using an Ohaus PA64 analytical balance. The mass yield of SOA was calculated from the extracted SOA mass, the air volume sampled, and the mass concentration of monoterpene reacted. Corrections for particle loss to the walls, which were ~15% h<sup>-1</sup>, were made using SMPS measurements as described elsewhere.<sup>33</sup> We did not attempt to correct yields for partitioning of gas phase products to the chamber walls. But the short period of reaction (1-4 min) compared to the  $\sim$ 10 min time scale for gas-wall partitioning 34,35 means that repartitioning of products from particles to the walls after the lights were turned off is indistinguishable from particle wall loss measured by the SMPS and so accounted for in that correction.

Derivatization-spectrophotometric methods<sup>22-24</sup> and an Agilent Cary 630 attenuated total reflectance Fourier-transform infrared spectrometer (ATR-FTIR) were used to characterize the functional group composition of SOA extracts. The derivatization-spectrophotometric methods quantify carbonyl (ketone and aldehyde), hydroxyl, carboxyl, ester, nitrate, and peroxide groups, the six major functional groups present in the SOA. For measurements of carbonyl, hydroxyl, carboxyl, and ester groups, a UV/vis-absorbing chromophore is attached by derivatization under conditions designed to drive the reaction to completion; <sup>23</sup> nitrate groups are measured using their strong UV/vis absorbance;<sup>36</sup> and peroxide groups are measured via irreversible I- oxidation to obtain a colored I<sub>3</sub>solution.<sup>22</sup> In the carbonyl, hydroxyl, carboxyl, and ester group analyses, two SOA samples were derivatized: one with an amount of derivatizing agent expected to be in excess of the amount of functional group present, and another with twice the amount. In all cases the amount of functional group measured in the two analyses was similar (within uncertainties), indicating that the functional groups were fully derivatized. Absorbance was measured using an Ocean Optics USB4000-UV/vis miniature fiber optic spectrophotometer with a 1 cm quartz cell. 3-Hexadecanone, 1,2-tetradecanediol, tridecanoic acid, bis(2-ethylhexyl) sebacate, and benzoyl peroxide were used as surrogate standards to generate calibration curves for quantifying carbonyl, hydroxyl, carboxyl, ester, and peroxide groups.<sup>22,23</sup> The use of these standards does not account for the impact of neighboring functional groups on the molar absorptivity of multifunctional compounds, but from analyses of a wide variety of compounds the resulting uncertainties have been estimated to be  $(\pm)$  10%, 20%, 20%, 30%, and 10% for carbonyl, hydroxyl, carboxyl, ester, and peroxide groups, respectively.<sup>22,23</sup> As discussed below, nitrate groups were quantified with an uncertainty of ±30% by using a range of molar absorptivities. Methylene (CH<sub>2</sub>) groups were quantified as the difference between the SOA mass and the total mass of all the measured functional groups.

Reversed-phase high-performance liquid chromatography (HPLC) with UV detection at 210 nm was used to fractionate SOA extracts. Measuring the absorbance at this wavelength allowed for specific detection and quantification of nitrate

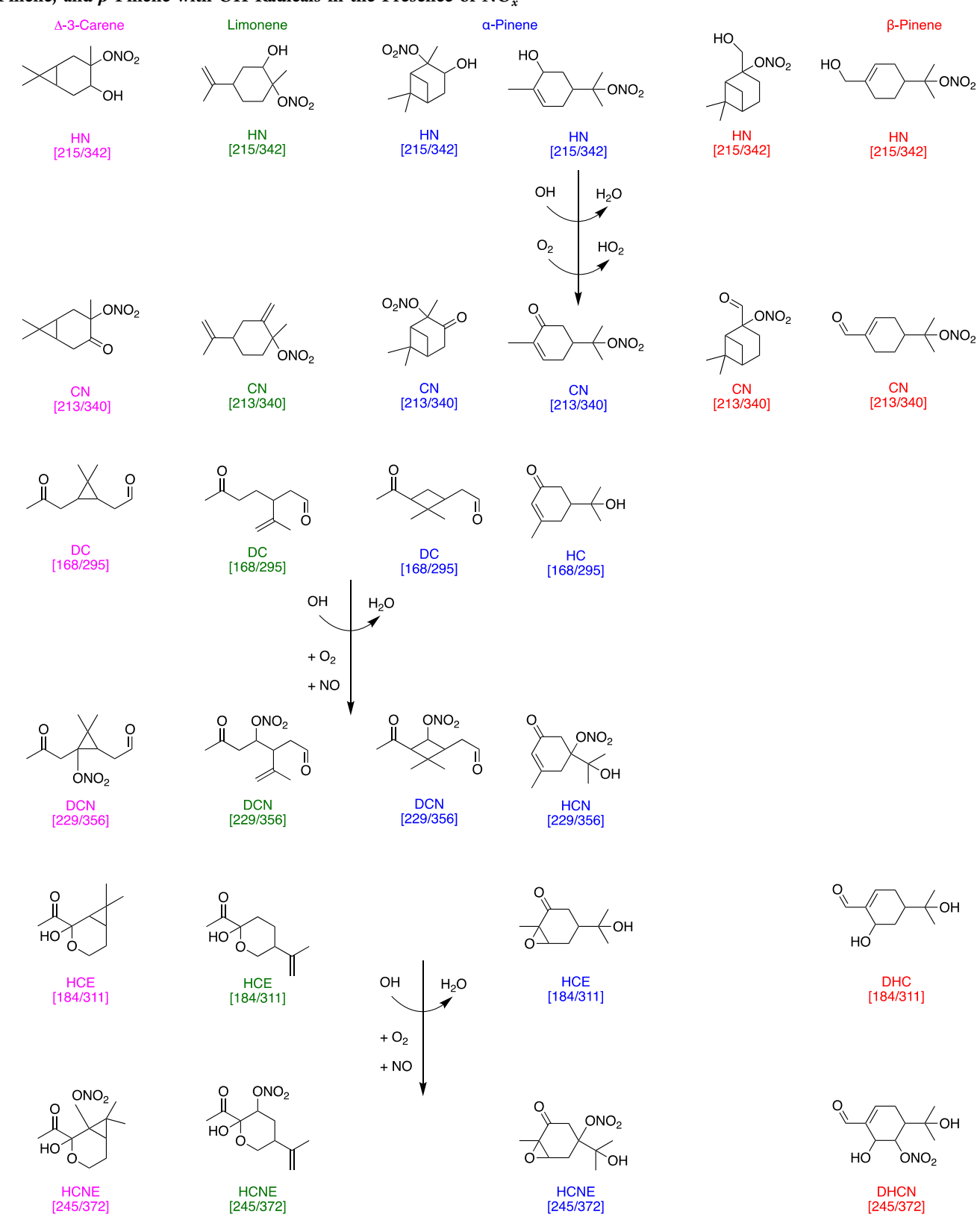
groups, which absorb much more strongly than any of the other functional groups.<sup>36</sup> This approach was used previously for analysis of organic nitrates in SOA formed from reactions of NO<sub>3</sub> radicals with these same monoterpenes. 15-17 The HPLC was a Shimadzu Prominence HPLC with a Zorbax Eclipse XDB-C18 column (250  $\times$  4.6 mm with 5  $\mu$ m particle size) and a Nexera X2 SPD-M30A UV/vis photodiode array detector, and a binary mobile phase gradient method was employed with mobile phase A being 95% water and 5% acetonitrile (v/v) and mobile phase B methanol, at a flow rate of 0.5 mL min<sup>-1</sup>. The method was as follows: 20% mobile phase B for 2 min, increase to 50% at 4.3% min<sup>-1</sup>, increase to 80% at 3% min<sup>-1</sup>, increase to 95% 0.75% min<sup>-1</sup>, hold at 95% for 20 min, increase to 100% at 1.7% min<sup>-1</sup>, and then hold at 100% for 10 min. Samples were collected manually after fractionation and then dried and concentrated to increase the signal obtained by subsequent analysis with an Agilent 6210 electrospray ionization-mass spectrometer (ESI-MS). Molecular weights of products were obtained from ESI-MS mass spectra, which consisted of Na+ adducts of molecules and sometimes a dimer cluster formed in the ESI source.

## ■ RESULTS AND DISCUSSION

Gas-Phase Reaction Mechanisms. Proposed mechanisms for forming first-generation products from gas-phase  $OH/NO_x$  reactions are shown in Scheme 1 for  $\Delta$ -3-carene, limonene, and ocimene; Scheme 2 for  $\alpha$ -pinene; and Scheme 3 for  $\beta$ -pinene. The acronym below each stable product designates the presence of hydroxyl (H), carbonyl (C), nitrate (N), ether (E), and ester (Es) groups, with (D) meaning di; and  $(\beta P-Ket)$ , (O-Ket), and (O-Ald) designate specific monofunctional ketones and aldehydes. Table S1 lists the names and corresponding acronyms for all the products. The numbers in brackets in Schemes 1-3 correspond to the compound molecular weight/I<sup>-</sup> adduct mass. Note that some products with different acronyms have the same molecular weight, since this value also depends on the number of rings and C=C bonds in the structure. The product assignments and proposed mechanisms were developed to be consistent with the gas-phase mass spectra and the results of our studies of reactions of these monoterpenes with  $NO_3$  radicals and 1-alkenes with  $OH/NO_{x^*}^{-15-19}$  They also drew significantly from the experimental and theoretical study by Xu et al.<sup>37</sup> and the theoretical studies of Peeters et al.<sup>38</sup> and Vereecken and Peeters<sup>39</sup> on the reactions of  $\alpha$ -pinene and  $\beta$ -pinene with OH/ NO<sub>x</sub>.

The reaction is initiated primarily by addition of an OH radical to a C=C bond to form a  $\beta$ -hydroxyalkyl radical, with H atom abstraction being ~10% or less. Under the conditions of these experiments, reactions with O<sub>3</sub> or NO<sub>3</sub> radicals are negligible since the 5 ppmv concentration of NO rapidly titrates both of these oxidants. For  $\Delta$ -3-carene,  $\alpha$ -pinene, and limonene, OH radicals add ~50:50 to either side of the C=C bond<sup>38,40</sup> (with the endoalkene site being the most reactive for limonene<sup>4,39</sup>), and for  $\beta$ -pinene addition is ~90:10 in favor of the formation of the tertiary  $\beta$ -hydroxyalkyl radical. <sup>25,39</sup> For ocimene, OH radicals add preferentially to the two methylsubstituted internal C=C bonds, with addition being about equally likely at either carbon, and because of conjugation the reaction also forms  $\delta$ -hydroxyalkyl radicals. <sup>4,25</sup>Schemes 1–3 show reaction mechanisms following OH radical addition at the most favorable site, but the other mechanisms are similar and significant differences are discussed.

Scheme 4. Proposed Second-Generation Gas-Phase  $C_{10}$  Products Formed from the Reaction of  $\Delta$ -3-Carene, Limonene,  $\alpha$ -Pinene, and  $\beta$ -Pinene with OH Radicals in the Presence of  $NO_x^a$ 



 $^a\mathrm{The}$  numbers in brackets correspond to the compound molecular weight/ $\mathrm{I}^-$  adduct mass.

For  $\Delta$ -3-carene, limonene, and ocimene the  $\beta$ -hydroxyalkyl radicals react solely with  $O_2$  to form  $\beta$ -hydroxyperoxy radicals. For  $\alpha$ -pinene and  $\beta$ -pinene, the secondary  $\beta$ -hydroxyalkyl

radicals also react solely by this pathway, whereas the tertiary  $\beta$ -hydroxyalkyl radicals also decompose by breaking open the 4-membered ring and then adding  $O_2$  to form  $(\text{non-}\beta)$ 

hydroxyperoxy radicals. Theory predicts that the branching between adding O2 and breaking open the 4-membered ring is ~30:70 for  $\alpha$ -pinene<sup>38</sup> and ~50:50 for  $\beta$ -pinene,<sup>39</sup> while measurements indicate values of ~40:60 and ~30:70.37 Under the conditions of our experiments the hydroxyperoxy radicals formed by all these pathways react solely with NO, since the rate of  $\sim 10^3 \text{ s}^{-1} (k_{\text{NO}} \times [\text{NO}] = 9 \times 10^{-12} \text{ cm}^3 \text{ molecule}^{-1} \text{ s}^{-14}$  $\times$  10<sup>14</sup> molecules cm<sup>-3</sup>) is much larger than rates of isomerization (<10 s<sup>-137</sup>), reaction with RO<sub>2</sub>· radicals (estimated concentration of  $\sim 10^8$  radicals cm<sup>-3</sup> for a steadystate production rate of ~1011 radicals cm<sup>-3</sup> s<sup>-1</sup> and loss by reaction with NO), and reactions with HO2 radicals present at similarly low concentrations. Reactions with NO will form hydroxynitrates (HN) or hydroxyalkoxy radicals. Our previous measurements of the branching ratios of reactions of hydroxyperoxy radicals with NO indicate that the yields of hydroxynitrates will be ~20%, with the other ~80% forming hydroxyalkoxy radicals.  $^{19,25}$  Although RO $_2\cdot$  radicals formed in our experiments (and in polluted atmospheres) will also react with NO<sub>2</sub> radicals to form peroxynitrates, ROONO<sub>2</sub>, because these compounds decompose reversibly on a time scale of a few seconds, 41 the RO<sub>2</sub> radicals will eventually react with NO.

The  $\beta$ -hydroxyalkoxy radicals formed in reactions of all the monoterpenes decompose by cleavage of the C-C bond between the alkoxy radical and hydroxyl groups to form the ring-opened C<sub>10</sub> dicarbonyls (DC) caronaldehyde, endolim (and 4-acetyl-1-methyl cyclohexene by decomposition of the other tertiary  $\beta$ -hydroxyalkoxy radical), and pinonaldehyde from  $\Delta$ -3-carene, limonene, and  $\alpha$ -pinene; the  $C_0$  ketone ( $\beta$ P-Ket) nopinone + formaldehyde from  $\beta$ -pinene; and 4-methyl-3-pentenal (O-Ald) + methyl vinyl ketone (O-Ket) from ocimene. For  $\Delta$ -3-carene and limonene the bond on the other side of the alkoxy radical group also breaks, whereas for  $\alpha$ pinene,  $\beta$ -pinene, and ocimene isomerization via an H shift or ring-closing reaction is more favorable. The alternative reaction with O<sub>2</sub> to form a carbonyl nitrate and HO<sub>2</sub> is too slow to compete with decomposition of all the  $\beta$ -hydroxyalkoxy radicals formed here, 42 as are reactions with NO to form a nitrite or with NO<sub>2</sub> to form a nitrate.<sup>25</sup> The alkyl radicals formed by decomposition of  $\beta$ -hydroxyalkoxy radicals react with O<sub>2</sub> to form hydroxycarbonyl, dihydroxy, or hydroxyether peroxy radicals; and in the case of  $\alpha$ -pinene a hydroxycarbonyl (HC) and HO<sub>2</sub>. These substituted alkylperoxy radicals then react with NO to form hydroxycarbonyl nitrates (HCN), dihydroxy nitrates (DHN), and hydroxynitrate ethers (HNE); or hydroxycarbonyl, dihydroxy, or hydroxyether alkoxy radicals that react by the pathways described above to form carbonylesters (CEs), hydroxydicarbonyls (HDC), dicarbonylesters (DCEs), dihydroxycarbonyl nitrates (DHCN), hydroxyearbonyl nitrate ethers (HCNE), and dihydroxycarbonyl nitrate ethers (DHCNE). The structures of HDC formed in reactions of  $\Delta$ -3-carene and limonene allow them to cyclize to hydroxycarbonyl ethers (HCE) (also called cyclic hemiacetals) in a few seconds either by collisions with particles<sup>43</sup> or in the gas phase by an HNO<sub>3</sub>-catalyzed reaction. 44 Some products formed in reactions of  $\alpha$ -pinene and  $\beta$ -pinene also have distant hydroxyl and carbonyl groups but are prevented from cyclizing by the strain the 6-membered ring.

Our results indicate that second-generation products were also formed in these experiments, since we were unable to explain some of the peaks in mass spectra based on first-generation products. Mechanisms proposed for forming second-generation products by H atom abstraction are

shown in Scheme 4. The reactions involve HN, DC, HC, HCE, and DHC products that are expected to be relatively abundant and exist primarily in the gas phase, where they are most accessible to reaction with OH radicals. Following H atom abstraction, HN alkyl radicals react with O<sub>2</sub> to form CN and HO<sub>2</sub>, while DC, HC, HCE, and DHC alkyl radicals add O<sub>2</sub> and then NO to form DCN, HCN, HCNE, and DHCN, respectively. Possible mechanisms for forming HCNEs and DCEs from secondary reactions of HCE are shown in Scheme S1.

The fractions of HN, DC, HC, HCE, and DHC predicted to undergo secondary OH radical reactions under the conditions of these experiments to form multifunctional nitrates were estimated by calculating the fraction of compound that undergoes H atom abstraction at sites that subsequently add O<sub>2</sub> to form an RO<sub>2</sub>· radical and then multiplying this value by a branching ratio for nitrate formation from reaction of the RO<sub>2</sub>. radical with NO. The first quantity was calculated using the equation given in Atkinson et al. 45 (which is based on consecutive reaction rate theory), the ratio of rate constants for the reaction of OH radicals with the first-generation product and the monoterpene, and the fraction of monoterpene remaining at the end of the reaction. Rate constants for the monoterpene reactions were taken from Atkinson and Arey,<sup>41</sup> and the rate constants used for the first-generation products were the sum of the partial rate constants for H atom abstraction at sites on HN, DC, HC, HCE, and DHC that lead to RO2· radicals that react with NO to form either a nitrate or alkoxy radical. Abstraction of an aldehydic H atom was not included since the subsequent reaction with O2 and then NO forms an acyloxy radical that decomposes by loss of CO<sub>2</sub>. The partial rate constants were calculated using the structure activity relationships in Ziemann and Atkinson.<sup>4</sup> The fraction of monoterpene remaining at the end of the reaction was 0.5 in all cases, as determined using the Vocus PTR-TOF measurements. The branching ratio for nitrate formation was taken to be 0.2, the value for C<sub>10</sub>n-alkanes. 46 From these calculations the average fraction of each of the following first-generation C<sub>10</sub> products that will react as shown in Scheme 4 are as follows: HN  $\rightarrow$  CN,  $\sim$ 0.4%; DC  $\rightarrow$  DCN and HC  $\rightarrow$  HCN, ~1.2%;  $\Delta$ -3-carene and limonene HCE  $\rightarrow$  HCNE, ~3.6%; and  $\beta$ -pinene and  $\alpha$ -pinene HCE and DHC  $\rightarrow$  HCNE and DHCN, ~1.2%. Assuming that the HN yields are ~20% (the same as those for C<sub>10</sub> acyclic 2-methyl-1-alkenes<sup>47</sup>) and that the yields of DC are ~30%, the estimated yields of CN and DCN are ~0.1% and ~0.4%.

Similar calculations give estimated fractions of HN  $\rightarrow$  DHDN reactions that occur by addition of OH radicals to C<sub>10</sub> HN C=C bonds (similar to the reactions that form HN in Schemes 1–3) that are ~4% for limonene and ocimene and ~2% for  $\alpha$ -pinene and  $\beta$ -pinene, assuming that ~50% of HN formed from  $\alpha$ -pinene and  $\beta$ -pinene have C=C bonds. <sup>37–39</sup> For HN yields of ~20%, <sup>46</sup> this gives DHDN yields of ~0.8% and ~0.4%, respectively. Since second-generation C<sub>4</sub> and C<sub>6</sub> HCN formed from reactions of O-Ket and O-Ald were detected in the ocimene mass spectrum, it is clear that C<sub>10</sub> DHDN are also formed in these reactions, but because they partition almost entirely to particles, they were not detected in I-CIMS mass spectra.

We note that the yields of CN, DHCN, and DHDN will be lower than the calculated values if a significant fraction of HN and HDC partition to the particles or walls on the time scale of the reactions. But since our previous measurements of gas-

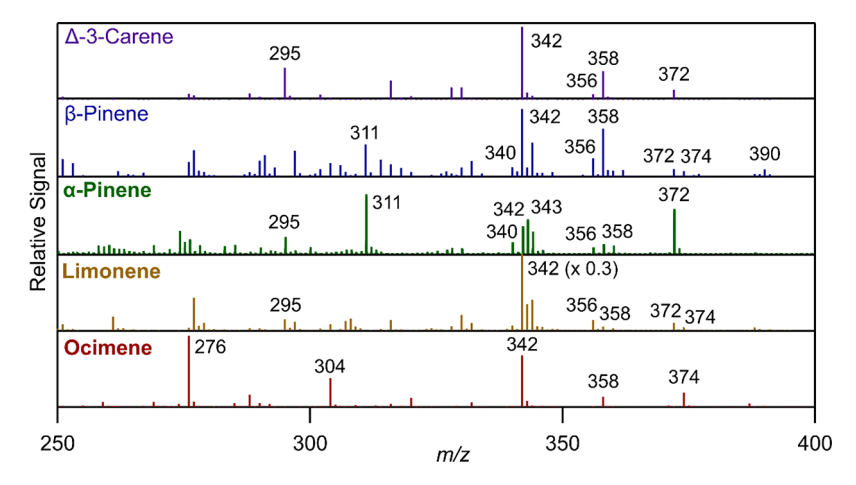


Figure 1. I-CIMS mass spectra measured in the mass range of monomers formed from the reactions of Δ-3-carene,  $\beta$ -pinene,  $\alpha$ -pinene, limonene, and ocimene with OH radicals in the presence of NO<sub>x</sub>. Signal for limonene's m/z 342 is multiplied by 0.3 to show presence of other peaks in the spectra.

particle partitioning of  $C_{10}$  HN formed from reactions of 1-alkenes with OH/NO $_x$  (which should be less volatile than those formed here since the hydroxyl and nitrate groups are primary and secondary) at SOA mass concentrations similar to those formed in these experiments indicated that only ~10% were present in particles, <sup>48</sup> and the ~10 min time scale for gaswall partitioning <sup>34,35</sup> is significantly longer than the 1–4 min duration of the reactions, most of the HN and HDC should be in the gas phase. Since the concentration of monoterpene reacted in each experiment was 0.5 ppmv, the estimated yields correspond to concentrations (ppbv) of HN ~ 100, DC ~ 150, CN ~ 0.5, DCN ~ 2, and DHDN ~ 2–4, indicating that all these products should be detectable in the I-CIMS.

Assignment of Gas-Phase Products. Mass spectra of the gas-phase reaction products measured with the I-CIMS are shown in Figure 1. The spectra are averages of the signal collected for 15-40 min after the reaction was initiated by turning on blacklights (which were on for  $\sim 90-240$  s), with the background signal measured prior to the reaction subtracted. All the spectra are normalized to the highest peak, except for limonene, for which the m/z 342 signal is multiplied but a factor of 0.3 so that smaller peaks are more visible. The reported masses are those of the I<sup>-</sup> adduct, which adds a nominal mass of 127 to the product molecular weight.

The observed and exact masses used to assign each product and the measurement mass accuracy are listed in Tables S2-S6, with mass accuracy defined in ppm units as  $10^6 \times$ (observed mass-exact mass)/exact mass. Note that all the detected products are monomers. The molecular formulas of various unassigned  $C_n$  (n < 10) products are listed in Table S7. Most of the products detected by the I-CIMS contained nitrate groups, with first-generation  $C_{10}$  HN (m/z 342) observed for all the monoterpenes, as was the case when they were reacted with NO<sub>3</sub> radicals. 17 Other assigned first-generation nitrates were C<sub>10</sub> HCN, HNE, and DHN (m/z 358); HCNE and DHCN (m/z 374); and DHCNE (m/z 390). Products assigned to second-generation nitrates were  $C_{10}$  CN (m/z)340); DCN and HCN (m/z 356); and DCHN and HCNE (m/z 372); and C<sub>4</sub> (m/z 276) and C<sub>6</sub> (m/z 304) HCN formed from O-Ket and O-Ald ocimene reaction products. The major assigned non-nitrate products were DC and HC (m/z 295); and HDC, DHC, and HCE (m/z 311). The m/z 295 peak is significant in the mass spectra of all the cyclic monoterpenes

(despite having a relatively low affinity for I compared to other products), except for  $\beta$ -pinene, because reaction at its exocyclic C=C bond leads to formation of  $\beta$ P-Ket and formaldehyde instead of DC, and its 4-membered ring-opening pathway does not lead to HC formation as with  $\alpha$ -pinene (Schemes 1 and 2). The m/z 311 peak in the  $\alpha$ -pinene and  $\beta$ pinene mass spectra is assigned to HCE and DHC formed via the 4-membered ring-opening pathways, and its absence in the  $\Delta$ -3-carene and limonene mass spectra indicates that the HDC formed in those reactions primarily cyclize to HCE, which then either react with OH radicals or have much lower I-CIMS sensitivity because of their structures. The other notable nonnitrate product peak is m/z 343. It is large in the  $\alpha$ -pinene spectrum but small in the others and corresponds to molecular formula C<sub>10</sub>C<sub>16</sub>O<sub>5</sub>. Although mechanisms could be developed to explain the formation of a corresponding product, since none of those we considered seemed sufficiently plausible we did not assign a product. We also note that the m/z 390 peak in the  $\beta$ -pinene mass spectrum is easily explained in the reaction mechanism, as is its absence in the other mass spectra, since no equally plausible mechanisms appear likely for those monoterpenes. It is a little surprising to observe this lowvolatility DHCNE in the gas phase, since no m/z 374 peak corresponding to HCNE is observed in the  $\alpha$ -pinene mechanism, apparently because it was primarily in the particles. Clearly, the sensitivity of the I-CIMS to the various products should be kept in mind when interpreting mass spectra. In addition, although the assigned structures are those we expect to be the dominant ones, structural isomers that we cannot distinguish with our methods will also be present. However, because they will most likely have been formed by the minor OH radical addition pathways not shown in the schemes and/or by alternative isomerization pathways involving H shift reactions at other carbon atoms, they will probably have similar structures and contain the same functional groups. Therefore, in spite of these uncertainties the good agreement between the proposed products and mass spectra provides strong support for the proposed gas-phase reaction mechanisms.

Functional Group Composition of SOA. After the SOA was extracted from the filters, ATR-FTIR spectra were measured to obtain qualitative information on functional groups. The spectra are shown in Figure 2, and they exhibit

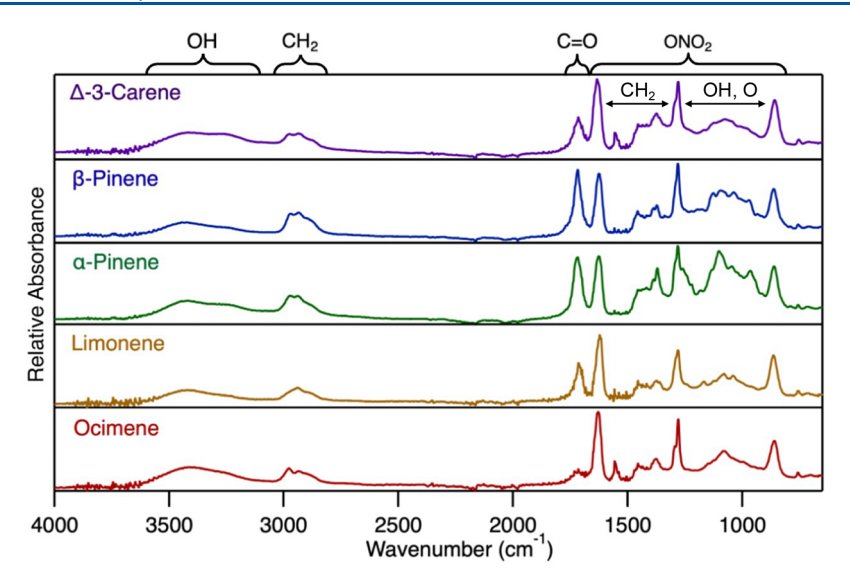


Figure 2. ATR-FTIR spectra of SOA formed from the reactions of Δ-3-carene,  $\beta$ -pinene,  $\alpha$ -pinene, limonene, and ocimene with OH radicals in the presence of NO<sub>x</sub>.

Table 1. Functional Group Composition and Related Properties of SOA Formed from the Reaction of  $\Delta$ -3-Carene,  $\beta$ -Pinene,  $\alpha$ -Pinene, Limonene, and Ocimene with OH Radicals in the Presence of NO<sub>x</sub> Determined by Derivatization-Spectrophotometric Analysis

	FG/C <sub>10</sub> molecule or related property <sup>a</sup>					
functional group or related property	Δ-3-carene	eta-pinene	lpha-pinene	limonene	ocimene	
nitrate [CHONO <sub>2</sub> ]	$1.0 \pm 0.3$	$0.6 \pm 0.2$	$1.0 \pm 0.3$	$1.0 \pm 0.3$	$1.6 \pm 0.5$	
carbonyl [C(O)]	$0.59 \pm 0.06$	$1.4 \pm 0.1$	$1.4 \pm 0.1$	$0.86 \pm 0.09$	$1.1 \pm 0.1$	
hydroxyl [CHOH]	$1.6 \pm 0.3$	$3.6 \pm 0.7$	$2.6 \pm 0.5$	$3.1 \pm 0.6$	$2.8 \pm 0.6$	
carboxyl $[C(O)OH]$	$0.11 \pm 0.02$	$0.14 \pm 0.03$	$0.23 \pm 0.05$	$0.02 \pm 0.01$	$0.08 \pm 0.02$	
ester $[C(O)OR]$	$0.27 \pm 0.08$	$0.5 \pm 0.1$	$0.5 \pm 0.1$	$0.3 \pm 0.1$	$0.3 \pm 0.1$	
peroxide [CHOOR]	$0.10 \pm 0.01$	$0.03 \pm 0.01$	$0.07 \pm 0.01$	$0.04 \pm 0.01$	$0.10 \pm 0.01$	
methylene [CH <sub>2</sub> ]	$6.4 \pm 0.3$	$3.8 \pm 0.3$	$4.2 \pm 0.3$	$4.7 \pm 0.3$	$4.1 \pm 0.3$	
O/C	$0.61 \pm 0.06$	$0.81 \pm 0.08$	$0.87 \pm 0.08$	$0.77 \pm 0.08$	$0.9 \pm 0.1$	
N/C	$0.10 \pm 0.03$	$0.06 \pm 0.02$	$0.10 \pm 0.03$	$0.10 \pm 0.03$	$0.16 \pm 0.05$	
H/C	$1.71 \pm 0.07$	$1.6 \pm 0.1$	$1.48 \pm 0.09$	$1.7 \pm 0.1$	$1.6 \pm 0.1$	
$M (g mol^{-1})$	$248 \pm 3$	$274 \pm 4$	$287 \pm 4$	$274 \pm 4$	$308 \pm 5$	
density (g cm <sup>-3</sup> )	$1.4 \pm 0.1$	$1.5 \pm 0.1$	$1.6 \pm 0.1$	$1.5 \pm 0.1$	$1.6 \pm 0.1$	

<sup>a</sup>Uncertainties listed for functional groups other than nitrate are based on relative standard deviations given in the text that were determined previously<sup>23</sup> for cases when multifunctional compounds are quantified using surrogate standards for calibrations. The uncertainty for the nitrate measurements are  $\pm 30\%$ , based on the range of molar absorptivities obtained previously when this method was applied to SOA formed from the reaction of Δ-3-carene with NO<sub>3</sub> radicals. <sup>16</sup> Other uncertainties were calculated by propagation of errors using the functional group uncertainties.

peaks associated with the major functional groups: nitrate (860, 1280, and 1625 cm<sup>-1</sup>), hydroxyl (1000–1300 and 3100–3600 cm<sup>-1</sup>), methylene and other groups with C–H bonds (1300–1500 and 2800–3000 cm<sup>-1</sup>), and carbonyl (1710–1740 cm<sup>-1</sup>). The assignment of these peaks is supported by the spectra shown in Figure S1 for liquid standards containing these functional groups. For comparison, Figure S1 includes a spectrum measured for SOA formed from the reaction of  $\beta$ -pinene with OH/NO<sub>x</sub>. Although the other functional groups contribute less to the SOA, note that ester and carboxyl groups also absorb at ~1710–1740 cm<sup>-1</sup>; ester, ether, and carboxyl groups also absorb in the 1000–1300 cm<sup>-1</sup> region (and in the methylene group regions), and carboxyl groups also absorb in the 3100–3600 cm<sup>-1</sup> region.

The assigned functional groups are also consistent with the products formed in the proposed gas-phase reaction mechanisms (Schemes 1–4). Nitrate groups are formed by radical chain terminating reactions of RO<sub>2</sub>· radicals with NO.

Carbonyl groups in ketones and aldehydes are formed directly by alkoxy radical decomposition via ring opening. They are also products (with  $HO_2$ ) of radical chain terminating reactions of  $O_2$  with  $\alpha$ -hydroxyalkyl radicals, which are formed by alkoxy radical decomposition, H shift isomerization reactions, and H atom abstraction from HN by OH radicals. Hydroxyl groups are formed by addition of OH radicals to C=C bonds and from alkoxy radical isomerization reactions.

The derivatization-spectrophotometric methods are more specific than ATR-FTIR analyses and also quantitative, but whereas an ATR-FTIR spectrum can be measured in a few minutes, derivatization-spectrophotometric analysis of a sample takes about 3 days. Here these methods were used to quantify nitrate, carbonyl (aldehyde and ketone), hydroxyl, carboxyl, ester, and peroxide functional groups in the SOA. The results are reported in Table 1 as the number of each functional group per  $C_{10}$  compound (with methylene groups assumed to comprise the remaining mass), where  $C_{10}$  was

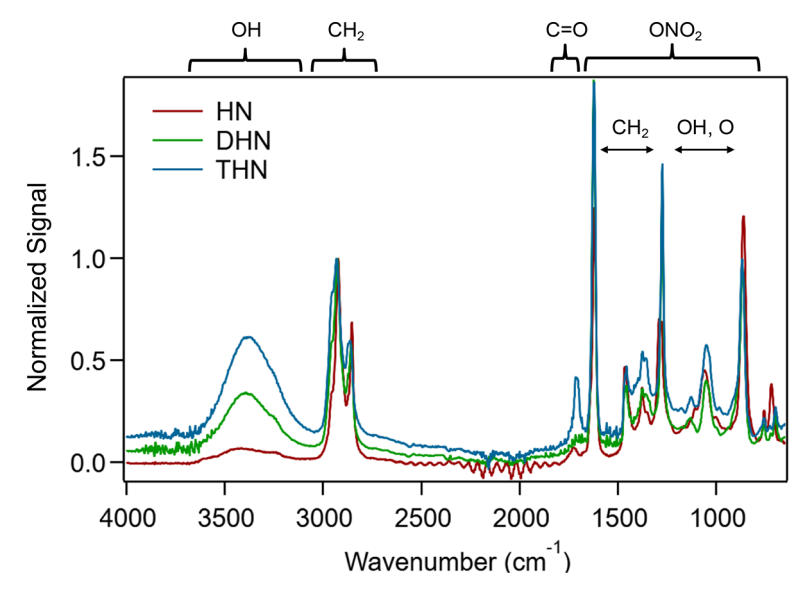


Figure 3. ATR-FTIR spectrum of hydroxynitrates (HN), dihydroxynitrates (DHN), and trihydroxynitrates (THN) formed from the reaction of 2-methyl-1-tridecene with OH radicals in the presence of  $NO_x$ . Spectra are normalized to the  $CH_2$  peak at  $\sim 3000$  cm<sup>-1</sup>. The small carbonyl peak is due to co-elution of another reaction product during the HPLC fractionation.

chosen because the parent monoterpenes all have 10 carbons. Uncertainties for all but the nitrate groups are based on previous measurements of the influence of multiple functional groups on compound absorbance.<sup>22,23</sup>

Nitrate groups were quantified from the absorbance measured at 210 nm, where nitrates have a natural absorbance that is orders of magnitude larger than that of any of the other functional groups.<sup>36</sup> The molar absorptivity of nitrate groups can vary significantly, however, depending on the molecular structure.  $^{19,23,25,30}$  To account for this, for  $\Delta$ -3-carene,  $\beta$ pinene,  $\alpha$ -pinene, and limonene we used an iterative process that is described elsewhere and begins with a molar absorptivity of a 2-ethylhexyl nitrate standard (3030 M<sup>-1</sup> cm<sup>-1</sup>). The final calculated molar absorptivities were 2480, 2575, 2554, and 2640 M<sup>-1</sup> cm<sup>-1</sup>, respectively. Because it was expected that secondary reactions led to a significant contribution of DHDN to the SOA formed in the ocimene reaction, which are not accounted for in the iterative process, for ocimene we used the average of these four values of 2560 M<sup>-1</sup> cm<sup>-1</sup>. The listed uncertainties for the nitrate measurements are ±30%, based on the range of molar absorptivities obtained previously when this method was applied to SOA formed from the reaction of  $\Delta$ -3-carene with NO<sub>3</sub> radicals. <sup>16</sup>

The range in the number of nitrate, carbonyl, hydroxyl, carboxyl, ester, and peroxide groups measured per  $C_{10}$  SOA product for the five monoterpenes were 0.6–1.6, 0.59–1.4, 1.6–3.6, 0.02–0.23, 0.27–0.5, and 0.03–0.1, with totals (1 – number of methylene groups) of 4.6, 6.2, 5.8, 5.3, and 5.9 for  $\Delta$ -3-carene,  $\beta$ -pinene,  $\alpha$ -pinene, limonene, and ocimene. The  $\sim$ 1 nitrate and  $\sim$ 1 carbonyl group per  $C_{10}$  SOA compound is consistent with the products shown in Schemes 1–4, whereas the  $\sim$ 2–4 hydroxyl groups is significantly higher.

Although we have not attempted to use the ATR-FTIR spectra to quantify the functional group composition of the SOA, it is still informative to compare ratios of peaks associated with different functional groups to evaluate their relative contributions to the SOA. For this reason, we chose standards for which the number of functional groups per 10 CH<sub>2</sub> groups is about the same as the number of functional

groups per  $C_{10}$  SOA compound measured in the derivatization-spectrophotometric analysis (except for the ester, since no liquid spectra were available for smaller esters). Comparing the ratio of the characteristic peak of a functional group to the  $CH_2$  peak at  $2800-3000~cm^{-1}$  for SOA and standards thus allows for a rough comparison of the number of functional groups. Average values of these functional group ratios (SOA/standard) are as follows: nitrate (1.0/1.3), carbonyl (1.1/1.1), hydroxyl (2.7/3.3), and ester (0.4/0.8) groups. It can also be useful to compare ratios of characteristic peaks of functional groups in SOA spectra.

For example, because the nitrate peaks are of similar intensity for all the monoterpenes, and the  $CH_2$  peak is largest for  $\beta$ -pinene, the spectra are consistent with SOA formed from the reaction of  $\beta$ -pinene having the smallest contribution from nitrate groups (0.6). It is not obvious that the  $CH_2$  peak is smallest for ocimene (though it might be), but because the estimated nitrate yields from secondary reactions were highest for ocimene it is reasonable that the SOA would have the largest contribution from nitrate groups (1.6). It is also worth noting that the ratio of any of the nitrate peaks relative to the  $CH_2$  peak is similar in all the SOA and the ethylhexyl nitrate standard, as might be expected since the ratio of nitrate to  $CH_2$  groups is  $\sim 1$  in all of them.

The smaller ratio of the carbonyl peak relative to the adjacent nitrate peak (which is easier to compare to than the CH<sub>2</sub> peak) in the  $\Delta$ -3-carene, limonene, and ocimene spectra compared to  $\beta$ -pinene and  $\alpha$ -pinene is consistent with the corresponding (carbonyl + ester)/nitrate ratios of 0.86, 1.16, and 0.88 compared to 3.2 and 1.9, respectively, measured by the derivatization-spectrophotometric methods. Although these differences could be due to larger contributions of carbonyl groups to SOA formed from reactions of  $\beta$ -pinene and  $\alpha$ -pinene, the more likely cause is that under the acidic conditions of the carbonyl functional group analysis the HCE formed in the  $\Delta$ -3-carene and limonene reactions (Scheme 1) reverted back to the acyclic HDC from which they were formed (as we have shown previously<sup>23</sup>), thus providing an additional carbonyl group for quantification that is not

Table 2. Average Functional Group Composition and Related Properties of SOA Formed from Reactions of Cyclic Monoterpenes ( $\Delta$ -3-Carene,  $\beta$ -Pinene,  $\alpha$ -Pinene, and Limonene) and an Acyclic Monoterpene (Ocimene) with OH/NO<sub>x</sub> and NO<sub>3</sub> Radicals Determined by Derivatization-Spectrophotometric Analysis

	FG/C <sub>10</sub> molecule or related property <sup>a</sup>					
	cyclic mor	noterpenes	acyclic mo	onoterpene		
functional group or related property	OH/NO <sub>x</sub>	NO <sub>3</sub>	OH/NO <sub>x</sub>	$NO_3$		
nitrate [CHONO <sub>2</sub> ]	$0.9 \pm 0.3$	$1.0 \pm 0.3$	$1.6 \pm 0.5$	$1.0 \pm 0.3$		
carbonyl [C(O)]	$1.1 \pm 0.1$	$0.38 \pm 0.03$	$1.1 \pm 0.1$	$0.60 \pm 0.06$		
hydroxyl [CHOH]	$2.7 \pm 0.5$	$0.06 \pm 0.01$	$2.8 \pm 0.6$	$0.35 \pm 0.07$		
carboxyl [C(O)OH]	$0.13 \pm 0.02$	$0.04 \pm 0.02$	$0.08 \pm 0.02$	$0.15 \pm 0.03$		
ester [C(O)OR]	$0.4 \pm 0.1$	$0.09 \pm 0.02$	$0.3 \pm 0.1$	$0.38 \pm 0.12$		
peroxide [CHOOR]	$0.06 \pm 0.01$	$0.05 \pm 0.01$	$0.10 \pm 0.01$	$0.24 \pm 0.01$		
methylene [CH <sub>2</sub> ]	$4.7 \pm 0.3$	$8.4 \pm 0.3$	$4.1 \pm 0.3$	$7.28 \pm 0.2$		
O/C	$0.77 \pm 0.08$	$0.38 \pm 0.06$	$0.9 \pm 0.1$	$0.55 \pm 0.06$		
N/C	$0.09 \pm 0.03$	$0.10 \pm 0.04$	$0.16 \pm 0.05$	$0.10 \pm 0.03$		
H/C	$1.60 \pm 0.09$	$1.80 \pm 0.06$	$1.6 \pm 0.1$	$1.70 \pm 0.05$		
M (g mol <sup>-1</sup> )	$271 \pm 4$	$213 \pm 3$	$308 \pm 5$	$238 \pm 2$		
density (g cm <sup>-3</sup> )	$1.5 \pm 0.1$	$1.29 \pm 0.08$	$1.6 \pm 0.1$	$1.33 \pm 0.08$		

<sup>a</sup>Uncertainties listed for functional groups other than nitrate are based on relative standard deviations given in the text that were determined previously<sup>23</sup> for cases when multifunctional compounds are quantified using surrogate standards for calibrations. The uncertainty for the nitrate measurements are  $\pm 30\%$ , based on the range of molar absorptivities obtained previously when this method was applied to SOA formed from the reaction of Δ-3-carene with NO<sub>3</sub> radicals. Other uncertainties were calculated by propagation of errors using the functional group uncertainties.

detected in the ATR-FTIR analysis. Acyclic products with similarly distant hydroxyl and carbonyl groups can also be formed from secondary reactions of ocimene products (not shown in Scheme 4), making cyclic hemiacetal formation possible there as well. Conversely, the carbonyl and hydroxyl groups in the products of the  $\beta$ -pinene and  $\alpha$ -pinene reactions are mostly prevented from reacting intramolecularly, either because of their close proximity or because of strain imposed by the 6-membered ring.

The 1.6-3.6 hydroxyl groups measured per C<sub>10</sub> SOA compound are generally higher than the number present in most of the products shown in Schemes 1-4, where the maximum is 2. Some of this discrepancy could be due to an effect of multiple functional groups on the absorbance that was not captured by the calibration standard and the uncertainties estimated from previous analyses of multifunctional alcohols.<sup>23</sup> However, the similarity in the ratio of the hydroxyl (3100-3600 cm<sup>-1</sup>) and CH<sub>2</sub> peaks in the SOA and alcohol standard also indicates  $\sim$ 3 hydroxyl groups per  $C_{10}$  compound. This is further supported by comparison of the SOA spectra with those shown in Figure 3 for C<sub>14</sub> hydroxynitrates, dihydroxynitrates, and trihydroxynitrates. These compounds, for which the ratios of the number of hydroxyl groups per 10 CH2 groups are 0.7, 1.4, and 2.1, were formed from the reaction of 2-methyl-1tridecene with OH/NO<sub>x</sub>, 30 collected as SOA, and then fractionated by HPLC prior to ATR-FTIR analysis.

One possibility is that the tertiary ether groups in the first-generation HCE, HCNE, HNE, DHCNE products, which are proposed to be formed to some extent in all the monoterpene reactions, are hydrolyzed in the SOA to form 2 hydroxyl groups according to the reaction  $R_3COCR_3 + H_2O \rightarrow R_3COH + R_3COH$ . This reaction has been shown to occur for methyl *tert*-butyl ether at pH  $\sim 1$  on a time scale of  $\sim 100$  h. <sup>50</sup> To determine if this reaction might be happening in SOA formed in our experiments, because of the presence of aqueous  $(NH_4)_2SO_4$  seed particles with pH  $\sim 1$  at 55% RH, and more rapidly because of the ditertiary-alkyl ether structure,  $\beta$ -pinene was also reacted in dry air without seed particles. The ATR-FTIR spectrum of the SOA shown in Figure S1 was then

collected for comparison. Because the spectrum is essentially identical to the one obtained for the original experimental conditions (Figure 2), it appears that either hydroxyl groups were not formed by this mechanism or that the seed particles and high RH are not necessary for the hydrolysis reactions to occur. It may be that these hydrolysis reactions do not require a catalyst, or that in the absence of the acidic seed particles the catalyst is HNO<sub>3</sub> formed from the NO<sub>2</sub> + OH → HNO<sub>3</sub> reaction that occurs in these experiments. As we have shown previously,<sup>51</sup> molecular HNO<sub>3</sub> formed in reactions of alkanes with OH/NO<sub>x</sub> acts as a general acid catalyst for the dehydration of cyclic hemiacetals with structures similar to those of HCE shown in Scheme 1 to form dihydrofurans. And its catalytic activity was much greater than that reported for dehydration via specific acid catalysis by H+. Catalysis by molecular HNO<sub>3</sub> may occur here under dry conditions (with enough water provided for hydrolysis even at RH < 1%), with H<sup>+</sup> catalysis dominating when acidic aqueous (NH<sub>4</sub>)<sub>2</sub>SO<sub>4</sub> seed particles are present at 55% RH. As discussed below, hydrolysis of products that contain tertiary nitrate groups can also add hydroxyl groups. But because most of the products formed in these reactions are first generation, which can have at most 1 nitrate group since nitrate formation terminates the reaction, the amount of nitrate hydrolysis required to add ~1 hydroxyl group per C<sub>10</sub> SOA compound would deplete the SOA of nearly all its nitrate groups. Since this is not the case, nitrate hydrolysis cannot explain the large number of hydroxyl groups in the SOA.

Formation of products containing the 0.27–0.5 ester groups per  $C_{10}$  compound measured in SOA are more difficult to plausibly explain than the other products. Possible mechanisms for forming first-generation DCEs and CEs esters in the reactions of  $\alpha$ -pinene and  $\beta$ -pinene are shown in Schemes 2 and 3, and possible mechanisms for forming second-generation HCNEs and DCEs esters from reactions of HCE products of the  $\Delta$ -3-carene and limonene reactions are shown in Figure S1. No similar mechanisms seem possible for forming esters in the reactions of ocimene. Unfortunately, the masses associated with these ester products are either absent or small in the I-

CIMS mass spectra (although the sensitivity of I-CIMS to ester and carbonyl groups is low) and all but the HCNEs are too volatile to contribute significantly to the SOA mass (Table S3). The source of ester groups in the SOA should therefore be viewed as an open question. This is also the case for the 0.02–0.23 carboxyl groups measured per  $C_{10}$  SOA compound, for which we offer no plausible mechanisms for product formation. The low peroxide content of the SOA is expected, since reactions with NO either convert peroxy radicals to alkoxy radicals or nitrates. The SOA peroxides are most likely second-generation acylperoxy nitrates formed when aldehydic H atoms are abstracted by OH radicals to form acyl radicals, followed by addition of  $O_2$  and then  $NO_2$ .

The SOA O/C, N/C, and H/C ratios; mean molecular weights; and densities are also included in Table 1. The elemental ratios were calculated by multiplying the tabulated values of FG/C<sub>10</sub> molecule by the number of O, N, H, and C atoms present in each functional group (shown in brackets), summing to obtain the total number of atoms of each element, and then using these values to calculate ratios. Densities were calculated from the elemental composition using an equation from Kuwata et al.<sup>52</sup> and the assumption that nitrogen has the same impact on density as oxygen. The O/C ratios of 0.6-0.9 are due mostly to nitrate and hydroxyl groups, which contribute 3 and 1 oxygens per functional group, respectively, and the N/C ratios of 0.6-1.6 are determined solely by nitrate groups. Average molecular weights and densities of 248-308 g mol<sup>-1</sup> and 1.4-1.6 compared to 136 and ~0.9 for monoterpenes also reflect the large numbers of functional groups.

These results can also be compared with those obtained by similar analysis of SOA formed from the reactions of the same monoterpenes with NO<sub>3</sub> radicals.<sup>17</sup> Averages for cyclic and acyclic monoterpenes formed from OH/NO<sub>x</sub> and NO<sub>3</sub> radical reactions are given in Table 2. The NO<sub>3</sub> reactions also create SOA products with  $\sim 1$  nitrate group per  $C_{10}$  compound, which is expected since the reaction is initiated by addition of an NO<sub>3</sub> radical to a C=C bond, and reactions were conducted with excess monoterpene so that formation of second-generation products was negligible. SOA formed in NO<sub>3</sub> radical reactions also have fewer carbonyl and hydroxyl groups because of formation of acetal dimers, which consume hydroxyl and carbonyl groups. Although some of the acetals are hydrolyzed under the acidic conditions of the carbonyl analysis, releasing carbonyl groups for quantification, this does not happen in the hydroxyl analysis. Numbers of other functional groups are similar for the two oxidants. As expected, because of the consumption of hydroxyl and carbonyl groups, average O/C ratios, densities, and molecular weights are much lower for NO<sub>3</sub> radical reactions, while N/C ratios are similar.

Yields of SOA and Organic Nitrates. The average SOA mass yields, measured for each of the monoterpenes in replicate experiments, were  $18 \pm 3$ ,  $55 \pm 8$ ,  $38 \pm 12$ ,  $57 \pm 6$ , and  $33 \pm 4\%$  for Δ-3-carene, β-pinene, α-pinene, limonene, and ocimene. When multiplied by the ratio of molecular weight of the monoterpene (136) and the average  $C_{10}$  product calculated from the measured functional group composition, the corresponding SOA molar yields are  $9 \pm 2$ ,  $27 \pm 4$ ,  $17 \pm 5$ ,  $29 \pm 3$ , and  $17 \pm 2\%$ . These yields are much lower than those measured for reactions with NO<sub>3</sub> radicals, where mass yields were 52, 81, 48, 78, and 69%, respectively. To comparison, SOA mass yields measured for reactions of the same cyclic monoterpenes and myrcene (which has a similar structure to

ocimene) with  $OH/NO_x$  were 38, 31, 32, 58, and 43%.<sup>53</sup> When multiplied by factors of  $\sim 1.1-1.3$  to account for the density of 1.25 assumed in those measurements compared to the higher values calculated here from the measured functional group composition (Table 1), the values increase to 43, 37, 41, 70, and 48%. The yields agree within factors of  $\sim 0.4-1.5$ , with this range probably being due to differences in reaction conditions such as light intensity; temperature; and monoterpene, OH radical, and  $NO_x$  concentrations.

The SOA molar yields can be multiplied by the number of nitrate groups per C<sub>10</sub> compound to obtain lower-limit estimates of the organic nitrate yields for each reaction, since this estimate only includes SOA products. As expected, because the number of nitrate groups per C<sub>10</sub> compound is  $\sim$ 1, these values are similar to the SOA molar yields. The resulting organic nitrate yields are  $9 \pm 2$ ,  $16 \pm 2$ ,  $17 \pm 5$ ,  $29 \pm 10$ 3, and 27  $\pm$  3% for reactions of  $\Delta$ -3-carene,  $\beta$ -pinene,  $\alpha$ pinene, limonene, and ocimene with OH/NO<sub>x</sub> compared to 32, 62, 35, 53, and 43% for reactions with NO<sub>3</sub> radicals, for which the SOA products also have ~1 nitrate group per C<sub>10</sub> compound. The higher values measured for the NO<sub>3</sub> radical reactions are due to the higher SOA yields, which we attribute to the large contribution of nonvolatile acetal and hemiacetal dimers formed by particle-phase accretion reactions to SOA formation.

Molecular Characterization of SOA Products. Chromatograms from the HPLC-UV analysis of SOA at 210 nm are presented in Figure 4. Because the derivatization-spectropho-

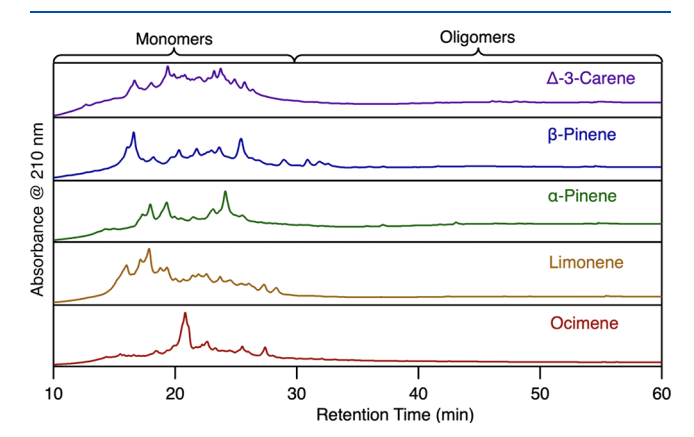


**Figure 4.** HPLC-UV chromatogram of SOA formed from the reactions of Δ-3-carene,  $\beta$ -pinene,  $\alpha$ -pinene, limonene, and ocimene with OH radicals in the presence of NO<sub>x</sub>.

tometric results indicate that nearly all the SOA products contain a nitrate group, this analysis is expected to detect the vast majority of products. The labels at the top of the chromatogram designate the regions where monomers and oligomers were expected to elute, based on the results of our previous studies of SOA formed from the reactions of the same monoterpenes with NO<sub>3</sub> radicals.  $^{15-17}$  In those studies,  $\sim$ 95% of the SOA products formed from the cyclic monoterpenes were present in the form of acetal and hemiacetal oligomers, and for  $\Delta$ -3-carene,  $\beta$ -pinene,  $\alpha$ -pinene, and limonene the HN/HCN acetal dimer comprised about 60, 54, 39, and 38% of the SOA. Despite observing both the HN and HCN monomers among the gas-phase products of the OH/NO<sub>x</sub> reactions, there are no signs of the HN/HCN dimer or any other nitrate oligomers in the chromatograms shown in Figure 4. In the case of  $\beta$ -pinene, the functional group analysis

indicates that only  $\sim\!60\%$  of the  $C_{10}$  SOA products contain a nitrate group, which suggests that the SOA also contained a significant mass of non-nitrate products. In order to determine whether non-nitrate products were eluting much later than the nitrate products as oligomers, fractions corresponding to peaks detected in the region before ~33 min (the time when the last nitrate product eluted) and the region after ~33 min were collected, dried, and weighed. The results indicated that about ~80% of the collected mass eluted before ~33 min and ~20% after, although the small amount of collected mass and contributions from solvent residue and other contaminants added considerable uncertainty to these measurements. Since it is likely that non-nitrate products eluted along with the nitrate products, these results are roughly consistent with the nitrate functional group analysis. It therefore appears that some non-nitrate products (including oligomers) were probably present in the SOA formed from the  $\beta$ -pinene reaction, although the quality of ATR-FTIR and ESI-MS spectra obtained for the small samples collected after ~33 min was insufficient to provide confirming information.

High-resolution ESI-MS analysis was also performed on HPLC-UV fractions collected in the monomer region of the chromatograms for SOA formed from reactions of all the monoterpenes. But unlike results from our previous analyses of the SOA products of the reactions of these monoterpenes with NO<sub>3</sub> radicals, 15-17 most mass spectra were apparently dominated by peaks derived from trace contaminants and could not be reasonably interpreted. This was the case regardless of whether the analyzed fraction was associated with a single peak or multiple peaks and was probably due to the high fraction of hydroxyl groups in these compounds, which ionize poorly in an ESI source. <sup>54</sup> By contrast, the acetal and hemiacetal dimers formed in NO3 radical reactions each contained two nitrate groups and few others. Because of the lack of useful information provided by most of the ESI/MS analyses (even for single peaks), no attempt was made to improve the chromatographic resolution by varying the gradient method. Nonetheless, by operating under the same conditions as in our previous studies, we were able determine whether the SOA products were monomers or oligomers by comparing retention times with those of dimers formed in the NO<sub>3</sub> radical reactions. The two mass spectra measured here that were sufficiently simple to provide useful information are discussed below. The molecular formulas, ions, and mass accuracies of SOA products detected by ESI-MS are given in Table S8.

The mass spectrum obtained from analysis of a fraction collected in the region containing the largest peak in the  $\beta$ pinene HPLC chromatogram (~15-18 min) is shown in Figure 5A. Peaks are present at m/z 286 and 407, which correspond to Na<sup>+</sup> adducts of mass 263 and 384 products, and also at m/z 549 and 791, which correspond to Na<sup>+</sup> adducts of homodimer clusters of these products that were formed in the ion source. The molecular formula of the mass 263 product is  $C_{10}H_{17}NO_{7}$ , which is assigned to DHCNE shown in Scheme 3. An m/z 390 peak corresponding to the I<sup>-</sup> adduct of this compound was observed in the I-CIMS mass spectrum, indicating that it was present in both the gas and particle phases. Its presence in the gas phase is surprising, since the five functional groups should lead to such a low vapor pressure that very little should be present in the gas phase. This suggests that I-CIMS is especially sensitive to this highly functionalized compound. The mass accuracy was insufficient to allow

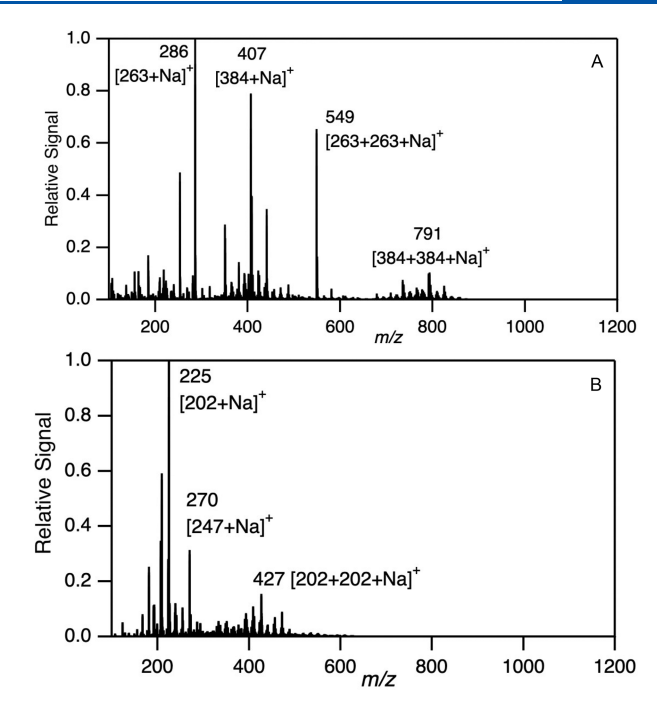


**Figure 5.** ESI-MS of HPLC fractions of SOA formed from the reactions of (A)  $\beta$ -pinene and (B) ocimene with OH radicals in the presence of NO<sub>x</sub>. The fractions analyzed in panels A and B were collected at ~15–18 and ~17–23 min, respectively.

confident assignment of a molecular formula to the mass 384 product, but since it is an even mass it is most likely either a  $C_x H_y O_z$  oligomer formed from fragmentation products or a contaminant.

The mass spectrum obtained from analysis of an SOA fraction collected in the region containing the largest peak in the ocimene HPLC chromatogram (~17-23 min) is shown in Figure 5B. The peaks at m/z 225 and 270 correspond to Na<sup>+</sup> adducts of products with nominal molecular weights of 202 and 247 and molecular formulas of C<sub>10</sub>H<sub>18</sub>O<sub>4</sub> and C<sub>10</sub>H<sub>17</sub>NO<sub>6</sub>, and the peak at m/z 427 is a Na<sup>+</sup> adduct of a homodimer cluster of the mass 202 product that was formed in the ion source. The C<sub>10</sub>H<sub>17</sub>NO<sub>6</sub> product is assigned to HCNE shown in Scheme 1. An m/z 374 peak corresponding to the I<sup>-</sup> adduct of this compound was observed in the I-CIMS mass spectrum, indicating that it was present in both the gas and particle phases. Detection of HCNE in the gas phase seems reasonable, while it is unsurprising that the less volatile DHCNE discussed above was not. A product with molecular formula C<sub>10</sub>H<sub>18</sub>O<sub>4</sub> is not included in the ocimene reaction mechanism, nor is a corresponding product observed in the I-CIMS spectrum. One interesting possibility is that it was formed by hydrolysis of the nitrate group in HCNE according to the reaction RONO<sub>2</sub> +  $H_2O \rightarrow ROH + HNO_3$ . This reaction would replace the nitrate group with a hydroxyl group, thus converting HCNE (molecular formula C<sub>10</sub>H<sub>17</sub>NO<sub>6</sub>) to DHCE (molecular formula C<sub>10</sub>H<sub>18</sub>O<sub>4</sub>). Evidence for this reaction comes from a recent study of the hydrolysis of organic nitrates formed from monoterpene oxidation, 55,56 which determined that the lifetimes of tertiary organic nitrates ranged from a few minutes to a few hours, depending on the compound structure and solution pH, while the lifetimes of secondary organic nitrates were ~10 days or more. This would explain the presence of DHCNE in the SOA formed in the  $\beta$ -pinene reaction, since it is a secondary nitrate (Scheme 3), while HCNE would be

hydrolyzed to DHCE because it is a tertiary nitrate (Scheme 1). The presence of both HCNE and DHCE in the SOA suggests that the lifetime is a few hours, comparable to the length of the chamber experiment, and near the upper end of the range of values measured in acidic aqueous solutions. St,56 Although some hydrolysis could also occur in the acetonitrile/water solution during HPLC analysis, this is less likely since the pH of the solution is close to neutral, much higher than the pH  $\sim$  1 of the seed particles, and the time available for reaction time was  $\sim$ 20 min compared to a few hours. Similar considerations apply to the other organic nitrates present in the SOA, but as discussed above, because the SOA products have an average of  $\sim$ 1 nitrate group per C<sub>10</sub> compound no significant amount of hydrolysis could have occurred during experiments, sample collection, storage, or analysis.

These results are also consistent with the fact that we have not seen any evidence for hydrolysis in our previous studies of the SOA formed from reactions of monoterpenes with NO $_3$  radicals, where acetal and hemiacetal nitrate oligomers that comprise  $\sim 95\%$  of the SOA are almost entirely secondary nitrates.  $^{15-17}$ 

Unfortunately, we do not have enough information about a number of factors to explain why hydrolysis of tertiary ethers (if it occurs) and nitrates appears to strongly favor ether hydrolysis, which seems to be necessary to explain the ~3 hydroxyl groups and  $\sim 1$  nitrate group per C<sub>10</sub> SOA compound measured by the functional group analysis. One unknown is the distribution of products within the SOA, which may be a phase-separated organic/aqueous mixture<sup>57</sup> or a single aqueous phase. This will affect the extent to which products are exposed to H<sup>+</sup> that can catalyze both reactions, since only a few percent of H<sup>+</sup> in the aqueous phase is expected to partition to the organic phase.<sup>58</sup> Although it is expected that the presence of tertiary ether and nitrate groups on the same molecule will increase the rate of the H<sup>+</sup> catalyzed reactions via resonance stabilization of the incipient carbocation, exactly how this will impact the competition between these reactions is also unknown. The same problem arises in understanding the effects of structure on possible general acid catalysis by HNO<sub>3</sub> under dry conditions.

# CONCLUSIONS

The results of this study provide insights into the gas- and particle-phase products and reaction mechanisms involved in the OH radical-initiated oxidation of cyclic and acyclic monoterpenes in the presence of NO<sub>x</sub>, conditions that are typical of a highly polluted environment. The products are almost entirely multifunctional, primarily containing various combinations of nitrate, carbonyl, hydroxyl, ester, and ether groups. They are mostly first-generation products formed in complex reactions that are initiated by addition of an OH radical to a C=C bond (creating a hydroxyl group), followed by radical reactions that involve a number of key competing pathways (which generally include reaction with O<sub>2</sub>) whose relative importance depends on the structure of the monoterpene. For cyclic alkyl radicals these include formation of cyclic RO<sub>2</sub>· radicals or decomposition to form ring opened RO<sub>2</sub>· radicals containing carbonyl groups; for RO<sub>2</sub>· radicals they include reaction with NO to form organic nitrates or alkoxy radicals + NO2; and for alkoxy radicals they include decomposition to form ring opened or fragment RO2· radicals or molecules, which both contain carbonyl groups, or isomerization via H shift or ring closing reactions that form

RO<sub>2</sub>· radicals containing hydroxyl or ether groups, respectively. The most volatile products react further via H atom abstraction by OH radicals to form second-generation products, and some that contain hydroxyl and carbonyl groups cyclize in particles to form cyclic hemiacetals.

The products and reaction mechanisms proposed here are consistent with the mass spectra obtained for gas-phase products and generally explain the similarities and differences observed among the cyclic monoterpenes and between the cyclic and acyclic monoterpenes. Results of analyses of SOA functional groups by quantitative derivatization-spectrophotometry and semiquantitative ATR-FTIR compare reasonably well with each other and provide complementary information since the first involves sample extraction and processing while the second does not. For the most part, the functional group analyses also agree with expectations based on the assignments of the structures of gas-phase products that formed the SOA, with the exception of a surprisingly large number of hydroxyl groups. The most likely explanation is that the tertiary ethers formed in these reactions are hydrolyzed in the SOA by a reaction that adds two hydroxyl groups to the product(s), but this could not be demonstrated.

Chromatograms of SOA analyzed by HPLC with UV detection indicate that the SOA is composed almost entirely of monomers, which is the opposite of what we observed previously for reactions of the same monoterpenes with NO<sub>3</sub> radicals. 15-17 There the SOA was composed almost entirely (>95%) of acetal and hemiacetal oligomers (mostly dimers) that were rapidly formed by particle-phase accretion reactions. The monomers were cyclic hemiacetals formed from HCN and similar compounds, which reacted with each other as well as HN and CN. A key structural feature of the monomers was the presence of a nitrate group adjacent to the carbonyl group in the HCN and CN, and adjacent to the hydroxyl groups in the cyclic hemiacetals and HN. Because of its electron-withdrawing ability, the nitrate group facilitates these reactions to the extent that they require no acid catalyst and occur in the presence of water, despite involving dehydration. Although HCN, HN, and CN are also formed in the OH/NO<sub>x</sub> reactions of these monoterpenes, hydroxyl and carbonyl groups are usually too close to each other or constrained by a ring to form cyclic hemiacetals, and most nitrate groups are not adjacent to carbonyl or hydroxyl groups. Another important distinction is that the nitrate groups in the oligomers formed in the NO<sub>3</sub> radical reactions are mostly secondary and so are stable toward hydrolysis, whereas the nitrate groups in ethers formed in the OH/NO<sub>r</sub> reactions are mostly tertiary and so can be rapidly hydrolyzed.  $^{55,56}$  The presence of  $\sim 1$  nitrate group and  $\sim 3$ hydroxyl groups per C<sub>10</sub> SOA compound indicates that in the competition between these reactions hydrolysis of ethers is favored.

As a result of low-volatility oligomer formation, the yields of SOA and organic nitrates were higher for NO<sub>3</sub> radical reactions than the OH/NO<sub>x</sub> reactions. For  $\Delta$ -3-carene,  $\beta$ -pinene,  $\alpha$ -pinene, limonene, and ocimene the average SOA mass yields were 52, 81, 48, 78, and 69% compared to 18, 55, 38, 57, and 33%, respectively. And the corresponding organic nitrate yields (which are lower limits since they only include SOA products) were 10, 16, 16, 25, and 21% compared to 32, 62, 35, 53, and 43%. It is clear from these results that relatively subtle differences in the structures of reaction products, even those with similar functional groups, can significantly impact SOA

formation and composition, which in turn affects aerosol properties such as volatility and hygroscopicity.

# ASSOCIATED CONTENT

# Supporting Information

The Supporting Information is available free of charge at https://pubs.acs.org/doi/10.1021/acs.jpca.2c04605.

Scheme for forming esters from secondary reactions of HCE; infrared spectra of SOA and standard compounds; tables of proposed reaction products and corresponding acronyms; ions and mass accuracies of gas-phase products detected by I-CIMS; nominal masses and molecular formulas of unassigned alkoxy radical decomposition products detected by I-CIMS; and molecular formulas, ions, and mass accuracies of SOA products detected by ESI-MS (PDF)

#### AUTHOR INFORMATION

## **Corresponding Author**

Paul J. Ziemann – Department of Chemistry, University of Colorado, Boulder, Colorado 80309, United States; Cooperative Institute for Research in Environmental Sciences (CIRES), Boulder, Colorado 80309, United States;

orcid.org/0000-0001-7419-0044; Phone: 303-492-9654; Email: paul.ziemann@colorado.edu

#### **Authors**

Marla P. DeVault – Department of Chemistry, University of Colorado, Boulder, Colorado 80309, United States; Cooperative Institute for Research in Environmental Sciences (CIRES), Boulder, Colorado 80309, United States

Anna C. Ziola – Department of Chemistry, University of

Anna C. Ziola – Department of Chemistry, University of Colorado, Boulder, Colorado 80309, United States; Cooperative Institute for Research in Environmental Sciences (CIRES), Boulder, Colorado 80309, United States

Complete contact information is available at: https://pubs.acs.org/10.1021/acs.jpca.2c04605

#### **Notes**

The authors declare no competing financial interest.

# ACKNOWLEDGMENTS

This material is based on work supported by the National Oceanic and Atmospheric Administration (NOAA) under Grant NA18OAR4310113 and by the National Science Foundation under Grant AGS-1750447.

## REFERENCES

- (1) Guenther, A. B.; Jiang, X.; Heald, C. L.; Sakulyanontvittaya, T.; Duhl, T.; Emmons, L. K.; Wang, X. The Model of Emissions of Gases and Aerosols from Nature Version 2.1 (MEGAN2.1): An Extended and Updated Framework for Modeling Biogenic Emissions. *Geosci. Model Dev.* 2012, 5, 1471–1492.
- (2) Atkinson, R.; Arey, J. Gas-Phase Tropospheric Chemistry of Biogenic Volatile Organic Compounds: A Review. *Atmos. Environ.* **2003**, *37*, 197–219.
- (3) Kroll, J. H.; Seinfeld, J. H. Chemistry of Secondary Organic Aerosol: Formation and Evolution of Low-Volatility Organics in the Atmosphere. *Atmos. Environ.* **2008**, *42*, 3593–3624.
- (4) Ziemann, P. J.; Atkinson, R. Kinetics, Products, and Mechanisms of Secondary Organic Aerosol Formation. *Chem. Soc. Rev.* **2012**, *41*, 6582–6605.

- (5) Zhang, Q.; Jimenez, J. L.; Canagaratna, M. R.; Allan, J. D.; Coe, H.; Ulbrich, I.; Alfarra, M. R.; Takami, A.; Middlebrook, A. M.; Sun, Y. L.; et al. Ubiquity and Dominance of Oxygenated Species in Organic Aerosols in Anthropogenically-influenced Northern Hemisphere Midlatitudes. *Geophys. Res. Lett.* 2007, 34, L13801.
- (6) de Gouw, J.; Jimenez, J. L. Organic Aerosols in the Earth's Atmosphere. *Environ. Sci. Technol.* **2009**, 43, 7614–7618.
- (7) Pöschl, U. Atmospheric Aerosols: Composition, Transformation, Climate and Health Effects. *Angew. Chem., Int. Ed.* **2005**, 44, 7520–7540
- (8) Perring, A. E.; Pusede, S. E.; Cohen, R. C. An Observational Perspective on the Atmospheric Impacts of Alkyl and Multifunctional Nitrates on Ozone and Secondary Organic Aerosol. *Chem. Rev.* **2013**, *113*, 5848–5870.
- (9) Rollins, A. W.; Browne, E. C.; Min, K.-E.; Pusede, S. E.; Wooldridge, P. J.; Gentner, D. R.; Goldstein, A. H.; Liu, S.; Day, D. A.; Russell, L. M.; et al. Evidence for  $NO_x$  Control over Nighttime SOA Formation. *Science* **2012**, 337, 1210–1212.
- (10) Ayres, B. R.; Allen, H. M.; Draper, D. C.; Brown, S. S.; Wild, R. J.; Jimenez, J. L.; Day, D. A.; Campuzano-Jost, P.; Hu, W.; de Gouw, J.; et al. Organic Nitrate Aerosol Formation via NO<sub>3</sub> + Biogenic Volatile Organic Compounds in the Southeastern United States. *Atmos. Chem. Phys.* **2015**, *15*, 13377–13392.
- (11) Xu, L.; Suresh, S.; Guo, H.; Weber, R. J.; Ng, N. L. Aerosol Characterization Over the Southeastern United States Using High-Resolution Aerosol Mass Spectrometry: Spatial and Seasonal Variation of Aerosol Composition and Sources with a Focus on Organic Nitrates. *Atmos. Chem. Phys.* **2015**, *15*, 7307–7336.
- (12) Pye, H. O. T.; Chan, A. W. H.; Barkley, M. P.; Seinfeld, J. H. Global Modeling of Organic Aerosol: The Importance of Reactive Nitrogen (NO<sub>x</sub> and NO<sub>3</sub>). *Atmospheric Chem. Phys.* **2010**, *10*, 11261–11276
- (13) Fisher, J. A.; Jacob, D. J.; Travis, K. R.; Kim, P. S.; Marais, E. A.; Chan Miller, C.; Yu, K.; Zhu, L.; Yantosca, R. M.; Sulprizio, M. P.; et al. Organic Nitrate Chemistry and Its Implications for Nitrogen Budgets in an Isoprene- and Monoterpene-Rich Atmosphere: Constraints from Aircraft (SEAC<sup>4</sup>RS) and Ground-Based (SOAS) Observations in the Southeast US. *Atmospheric Chem. Phys.* **2016**, *16*, 5969–5991.
- (14) Ng, N. L.; Brown, S. S.; Archibald, A. T.; Atlas, E.; Cohen, R. C.; Crowley, J. N.; Day, D. A.; Donahue, N. M.; Fry, J. L.; Fuchs, H.; et al. Nitrate Radicals and Biogenic Volatile Organic Compounds: Oxidation, Mechanisms, and Organic Aerosol. *Atmospheric Chem. Phys.* **2017**, *17*, 2103–2162.
- (15) Claflin, M. S.; Ziemann, P. J. Identification and Quantitation of Aerosol Products of the Reaction of  $\beta$ -Pinene with NO<sub>3</sub> Radicals and Implications for Gas- and Particle-Phase Reaction Mechanisms. *J. Phys. Chem. A* **2018**, *122*, 3640–3652.
- (16) DeVault, M. P.; Ziemann, P. J. Gas- and Particle-Phase Products and Their Mechanisms of Formation from the Reaction of  $\Delta$ -3-Carene with NO<sub>3</sub> Radicals. *J. Phys. Chem. A* **2021**, *125*, 10207–10222.
- (17) DeVault, M. P.; Ziola, A. C.; Ziemann, P. J. Products and Mechanisms of Secondary Organic Aerosol Formation from the NO<sub>3</sub> Radical-Initiated Oxidation of Cyclic and Acyclic Monoterpenes. *ACS Earth Space Chem.* **2022**, *6*, 2076–2092.
- (18) Matsunaga, A.; Docherty, K. S.; Lim, Y. B.; Ziemann, P. J. Composition and Yields of Secondary Organic Aerosol Formed from OH Radical-Initiated Reactions of Linear Alkenes in the Presence of NO<sub>x</sub>: Modeling and Measurements. *Atmos. Environ.* **2009**, 43, 1349–1357.
- (19) Bakker-Arkema, J. G.; Ziemann, P. J. Comprehensive Analysis of Products and the Development of a Quantitative Mechanism for the OH Radical-Initiated Oxidation of 1-Alkenes in the Presence of NO<sub>x</sub>. J. Phys. Chem. A **2021**, 125, 5829–5840.
- (20) Bruckner, R. Advanced Organic Chemistry, 1st ed.; Harcourt/Academic Press: San Diego, CA, 2002.
- (21) Taylor, W. D.; Allston, T. D.; Moscato, M. J.; Fazekas, G. B.; Kozlowski, R.; Takacs, G. A. Atmospheric Photodissociation Lifetimes

- for Nitromethane, Methyl Nitrite, and Methyl Nitrate. Int. J. Chem. Kinet. 1980, 12, 231–240.
- (22) Docherty, K. S.; Wu, W.; Lim, Y. B.; Ziemann, P. J. Contributions of Organic Peroxides to Secondary Aerosol Formed from Reactions of Monoterpenes with O<sub>3</sub>. *Environ. Sci. Technol.* **2005**, 39, 4049–4059.
- (23) Aimanant, S.; Ziemann, P. J. Development of Spectrophotometric Methods for the Analysis of Functional Groups in Oxidized Organic Aerosol. *Aerosol Sci. Technol.* **2013**, *47*, 581–591.
- (24) Claflin, M.; Liu, J.; Russell, L. M.; Ziemann, P. J. Comparison of Methods of Functional Group Analysis Using Results from Laboratory and Field Aerosol Measurements. *Aerosol Sci. Technol.* **2021**, *55*, 1042–1058.
- (25) Bakker-Arkema, J. G.; Ziemann, P. J. Minimizing Errors in Measured Yields of Particle-Phase Products Formed in Environmental Chamber Reactions: Revisiting the Yields of  $\beta$ -Hydroxynitrates Formed from 1-Alkene + OH/NO<sub>x</sub> Reactions. ACS Earth Space Chem. **2021**, *5*, 690–702.
- (26) Gao, Y.; Chen, S. B.; Yu, L. E. Efflorescence Relative Humidity of Ammonium Sulfate Particles. *J. Phys. Chem. A* **2006**, *110*, 7602–7608.
- (27) Pye, H. O. T.; Nenes, A.; Alexander, B.; Ault, A. P.; Barth, M. C.; Clegg, S. L.; Collett, J. L., Jr.; Fahey, K. M.; Hennigan, C. J.; Herrmann, H.; et al. The Acidity of Atmospheric Particles and Clouds. *Atmos. Chem. Phys.* **2020**, *20*, 4809–4888.
- (28) Nault, B. A.; Campuzano-Jost, P.; Day, D. A.; Jo, D. S.; Schroder, J. C.; Allen, H. M.; Bahreini, R.; Bian, H.; Blake, D. R.; Chin, M.; et al. Chemical Transport Models Often Underestimate Inorganic Aerosol Acidity in Remote Regions of the Atmosphere. *Commun. Earth Environ.* 2021, 2, 93.
- (29) Atkinson, R.; Carter, W. P. L.; Winer, A. M.; Pitts, J. N., Jr. An Experimental Protocol for the Determination of OH Radical Rate Constants with Organics Using Methyl Nitrite Photolysis as an OH Radical Source. J. Air Pollut. Control Assoc. 1981, 31, 1090–1092.
- (30) Matsunaga, A.; Ziemann, P. J. Yields of  $\beta$ -Hydroxynitrates, Dihydroxynitrates, and Trihydroxynitrates Formed from OH Radical-Initiated Reactions of 2-Methyl-1-Alkenes. *Proc. Natl. Acad. Sci. U. S. A.* **2010**, *107*, 6664–6669.
- (31) Krechmer, J. E.; Groessl, M.; Zhang, X.; Junninen, H.; Massoli, P.; Lambe, A. T.; Kimmel, J. R.; Cubison, M. J.; Graf, S.; Lin, Y.-H.; et al. Ion Mobility Spectrometry-Mass Spectrometry for On- and Off-Line Analysis of Atmospheric Gas and Aerosol Species. *Atmos. Meas. Technol.* 2016, *9*, 3245–3262.
- (32) Krechmer, J.; Lopez-Hilfiker, F.; Koss, A.; Hutterli, M.; Stoermer, C.; Deming, B.; Kimmel, J.; Warneke, C.; Holzinger, R.; Jayne, J.; et al. Evaluation of a New Reagent Ion Source and Focusing Ion—Molecule Reactor for Use in Proton-Transfer-Reaction Mass Spectrometry. *Anal. Chem.* **2018**, *90*, 12011–12018.
- (33) Yeh, G. K.; Claflin, M. S.; Ziemann, P. J. Products and Mechanism of the Reaction of 1-Pentadecene with NO<sub>3</sub> Radicals and the Effect of a ONO<sub>2</sub> Group on Alkoxy Radical Decomposition. *J. Phys. Chem. A* **2015**, *119*, 10684–10696.
- (34) Matsunaga, A.; Ziemann, P. J. Gas-Wall Partitioning of Organic Compounds in a Teflon Film Chamber and Potential Effects on Reaction Product and Aerosol Yield Measurements. *Aerosol Sci. Technol.* **2010**, *44*, 881–892.
- (35) Krechmer, J. E.; Pagonis, D.; Ziemann, P. J.; Jimenez, J. L. Quantification of Gas-Wall Partitioning in Teflon Environmental Chambers Using Rapid Bursts of Low-Volatility Oxidized Species Generated In Situ. *Environ. Sci. Technol.* **2016**, *50*, 5757–5765.
- (36) Docherty, K. S.; Ziemann, P. J. Reaction of Oleic Acid Particles with NO<sub>3</sub> Radicals: Products, Mechanism, and Implications for Radical-Initiated Organic Aerosol Oxidation. *J. Phys. Chem. A* **2006**, 110. 3567–3577.
- (37) Xu, L.; Møller, K. H.; Crounse, J. D.; Otkjær, R. V.; Kjaergaard, H. G.; Wennberg, P. O. Unimolecular Reactions of Peroxy Radicals Formed in the Oxidation of  $\alpha$ -Pinene and  $\beta$ -Pinene by OH Radicals. *J. Phys. Chem. A* **2019**, *123*, 1661–1674.

- (38) Peeters, J.; Vereecken, L.; Fantechi, G. The Detailed Mechanism of the OH-Initiated Atmospheric Oxidation of  $\alpha$ -Pinene: A Theoretical Study. *Phys. Chem. Chem. Phys.* **2001**, 3, 5489–5504.
- (39) Vereecken, L.; Peeters, J. A Theoretical Study of the OH-Initiated Gas-Phase Oxidation Mechanism of  $\beta$ -Pinene (C10H16): First Generation Products. *Phys. Chem. Chem. Phys.* **2012**, *14*, 3802–3815.
- (40) Atkinson, R.; Arey, J. Atmospheric Degradation of Volatile Organic Compounds. *Chem. Rev.* **2003**, *103*, 4605–4638.
- (41) Orlando, J. J.; Tyndall, G. S. Laboratory Studies of Organic Peroxy Radical Chemistry: An Overview with Emphasis on Recent Issues of Atmospheric Significance. *Chem. Soc. Rev.* **2012**, *41*, 6294–6317
- (42) Atkinson, R. Rate Constants for the Atmospheric Reactions of Alkoxy Radicals: An Updated Estimation Method. *Atmos. Environ.* **2007**, *41*, 8468–8485.
- (43) Lim, Y. B.; Ziemann, P. J. Kinetics of the Heterogeneous Conversion of 1,4-Hydroxycarbonyls to Cyclic Hemiacetals and Dihydrofurans on Organic Aerosol Particles. *Phys. Chem. Chem. Phys.* **2009**, *11*, 8029–8039.
- (44) Arathala, P.; Tangtartharakul, C. B.; Sinha, A. Atmospheric Ring-Closure and Dehydration Reactions of 1,4-Hydroxycarbonyls in the Gas Phase: The Impact of Catalysts. *J. Phys. Chem. A* **2021**, *125*, 5963–5975.
- (45) Atkinson, R.; Aschmann, S. M.; Carter, W. P. L.; Winer, A. M.; Pitts, J. N., Jr. Alkyl Nitrate Formation from the Nitrogen Oxide (NO<sub>x</sub>)-Air Photooxidations of  $C_2$ – $C_8$  n-Alkanes. *J. Phys. Chem.* **1982**, 86, 4563–4569.
- (46) Yeh, G. K.; Ziemann, P. J. Alkyl Nitrate Formation from the Reactions of  $C_8-C_{14}$ n-Alkanes with OH Radicals in the Presence of NOx: Measured Yields with Essential Corrections for Gas–Wall Partitioning. *J. Phys. Chem. A* **2014**, *118*, 8147–8157.
- (47) Matsunaga, A.; Ziemann, P. J. Branching Ratios and Rate Constants for Decomposition and Isomerization of β-Hydroxyalkoxy Radicals Formed from OH Radical-Initiated Reactions of  $C_6$ – $C_{13}$  2-Methyl-1-Alkenes in the Presence of NO<sub>x</sub>. *J. Phys. Chem. A* **2019**, *123*, 7839–7846.
- (48) Matsunaga, A.; Ziemann, P. J. Yields of  $\beta$ -Hydroxynitrates and Dihydroxynitrates in Aerosol Formed from OH Radical-Initiated Reactions of Linear Alkenes in the Presence of NO<sub>x</sub>. *J. Phys. Chem. A* **2009**, *113*, 599–606.
- (49) Riva, M.; Rantala, P.; Krechmer, J. E.; Perakyla, O.; Zhang, Y.; Heikkinen, L.; Garmasn, O.; Yan, C.; Kulmala, M.; Worsnop, D.; et al. Evaluating the Performance of Five Different Chemical Ionization Techniques of Detecting Gaseous Oxygenated Organic Species. *Atmos. Meas. Technol.* **2019**, *12*, 2403–2421.
- (50) O'Reilly, K. T.; Moir, M. R.; Taylor, C. D.; Smith, C. A.; Hyman, M. R. Hydrolysis of *tert*-Butyl Methyl Ether (MTBE) in Dilute Aqueous Acid. *Environ. Sci. Technol.* **2001**, *35*, 3954–3961.
- (51) Ranney, A. P.; Ziemann, P. J. Kinetics of Acid-Catalyzed Dehydration of Cyclic Hemiacetals in Aerosol Particles in Equilibrium with Nitric Acid Vapor. *J. Phys. Chem. A* **2016**, *120*, 2561–2568.
- (52) Kuwata, M.; Zorn, S. R.; Martin, S. T. Using Elemental Ratios to Predict the Density of Organic Material Composed of Carbon, Hydrogen, and Oxygen. *Environ. Sci. Technol.* **2012**, *46*, 787–794.
- (53) Lee, A.; Goldstein, A. H.; Kroll, J. H.; Ng, N. L.; Varutbangkul, V.; Flagan, R. C.; Seinfeld, J. H. Gas-Phase Products and Secondary Aerosol Yields from the Photooxidation of 16 Different Terpenes. *J. Geophys. Res.* **2006**, *111*, D17305.
- (54) Johnson, D. W. Analysis of Alcohols, as Dimethylglycine Esters, by Electrospray Ionization Tandem Mass Spectrometry. *J. Mass Spectrom.* **2001**, *36*, 277–283.
- (55) Rindelaub, J. D.; Borca, C. H.; Hostetler, M. A.; Slade, J. H.; Lipton, M. A.; Slipchenko, L. V.; Shepson, P. B. The Acid-Catalyzed Hydrolysis of a-Pinene-Derived Organic Nitrate: Kinetics, Products, Reaction Mechanisms, and Atmospheric Impact. *Atmos. Chem. Phys.* **2016**, *16*, 15425–15432.
- (56) Wang, Y.; Piletic, I. R.; Takeuchi, M.; Xu, T.; France, S.; Ng, N. L. Synthesis and Hydrolysis of Atmospherically Relevant Mono-

terpene-Derived Organic Nitrates. Environ. Sci. Technol. 2021, 55, 14595–14606.

- (57) Bertram, A. K.; Martin, S. T.; Hanna, S. J.; Smith, M. L.; Bodsworth, A.; Chen, Q.; Kuwata, M.; Liu, A.; You, Y.; Zorn, S. R. Predicting the Relative Humidities of Liquid-Liquid Phase Separation, Efflorescence, and Deliquescence of Mixed Particles of Ammonium Sulfate, Organic Material, and Water Using the Organic-to-Sulfate Mass Ratio of the Particle and the Oxygen-to-Carbon Elemental Ratio of the Organic Component. *Atmos. Chem. Phys.* **2011**, *11*, 10995–1100.
- (58) Deming, B. L.; Ziemann, P. J. Measurements of the Partitioning of Nitric Acid and Sulfuric Acid in Aqueous/Organic Phase-Separated Systems. *Environ. Sci. Atmos.* **2021**, *1*, 93–103.

# **Supporting Information**

Chemistry of Secondary Organic Aerosol Formation from Reactions of Monoterpenes with OH Radicals in the Presence of NO<sub>x</sub>

Marla P. DeVault<sup>†,‡</sup>, Anna C. Ziola<sup>†,‡</sup>, and Paul J. Ziemann<sup>†,‡,\*</sup>

- † Cooperative Institute for Research in Environmental Sciences (CIRES), Boulder, Colorado 80309, United States
- ‡ Department of Chemistry, University of Colorado, Boulder, Colorado 80309, United States

**Abstract.** Scheme for forming esters from secondary reactions of HCE (Scheme S1); figure of infrared spectra of standard compounds (Figure S1); tables of proposed reaction products and corresponding acronyms (Table S1); molecular formulas, ions, and mass accuracies of gas-phase products detected by I-CIMS (Tables S2–S6); nominal masses and molecular formulas of unassigned alkoxy radical decomposition products detected by I-CIMS (Table S7); and molecular formulas, ions, and mass accuracies of SOA products detected by ESI-MS (Table S8).

**Scheme S1.** Proposed mechanisms for forming esters from secondary reactions of HCE.

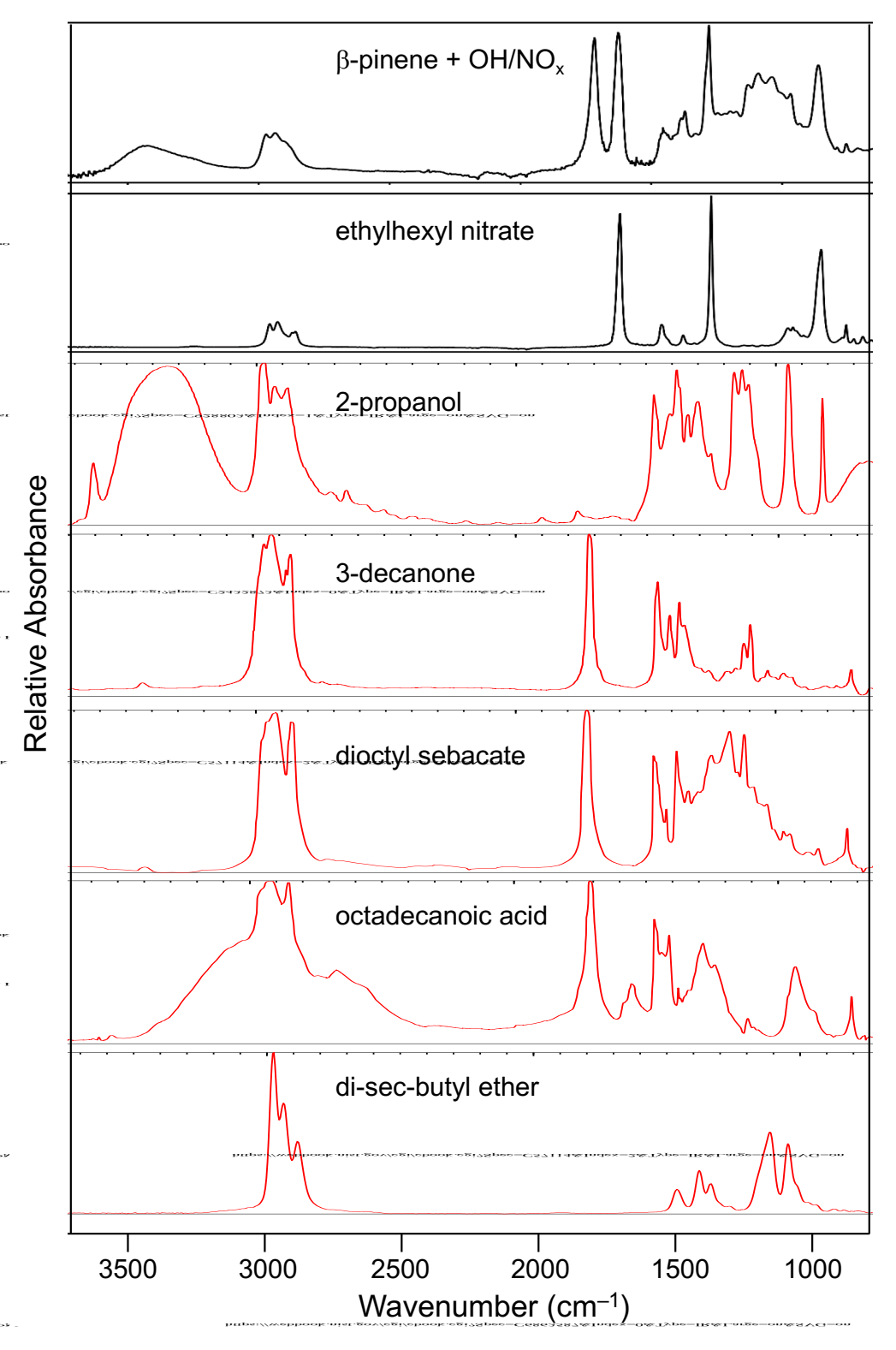


**Figure S1.** ATR-FTIR spectra of SOA formed from the reaction of  $\beta$ -pinene with NO<sub>x</sub>, and liquid ethylhexyl nitrate, and infrared spectra of standards in measured in solution and downloaded from Evaluated Infrared Spectra, Coblentz Society, Inc., NIST Standard Reference Database Number 69, NIST Chemistry WebBook.

 Table S1. Proposed reaction products and corresponding acronyms.

Product Name	Product Acronym
β-Pinene ketone	βP-Ket
Ocimene aldehyde	O-Ald
Ocimene ketone	O-Ket
Dicarbonyl	DC
Hydroxynitrate	HN
Carbonyl ester	CEs
Hydroxydicarbonyl	HDC
Dihydroxycarbonyl	DHC
Dihydroxynitrate	DHN
Hydroxycarbonyl ether	НСЕ
Hydroxynitrate ether	HNE
Dicarbonyl ester	DCEs
Hydroxycarbonyl nitrate ether	HCNE
Dihydroxycarbonyl nitrate	DHCN
Dihydroxycarbonyl nitrate ether	DHCNE

**Table S2.** Molecular formulas, ions, and mass accuracies of assigned gas-phase products detected by I-CIMS in the reactions of  $\Delta$ -3-carene with OH radicals in the presence of NO<sub>x</sub>.

Molecular Formula	Ion	Exact Mass (Da)	Observed Mass (Da)	Mass Accuracy (ppm)
$C_{10}H_{16}O_{2}$	[M+I] <sup>-</sup>	295.01950	295.02003	1.8
$C_{10}H_{16}O_3$	[M+I] <sup>-</sup>	311.01441	311.01504	2.0
$C_{10}H_{17}NO_4\\$	[M+I] <sup>-</sup>	342.02023	342.02074	1.5
$C_{10}H_{15}NO_5\\$	[M+I] <sup>-</sup>	355.99949	355.99982	0.9
$C_{10}H_{17}NO_5$	[M+I] <sup>-</sup>	358.01514	358.01557	1.2
$C_{10}H_{15}NO_6$	[M+I] <sup>-</sup>	371.99441	371.99483	1.1

**Table S3.** Molecular formulas, ions, and mass accuracies of assigned gas-phase products detected by I-CIMS in the reaction of  $\beta$ -pinene with OH radicals in the presence of  $NO_x$ .

Molecular Formula	Ion	Exact Mass (Da)	Observed Mass (Da)	Mass Accuracy (ppm)
$C_{10}H_{16}O_3$	[M+I] <sup>-</sup>	311.01441	311.01474	1.0
$C_{10}H_{15}NO_4\\$	[M+I] <sup>-</sup>	340.00513	340.00492	-0.6
$C_{10}H_{17}NO_4\\$	$[M+I]^-$	342.02023	342.02065	1.2
$C_{10}H_{15}NO_5\\$	[M+I] <sup>-</sup>	355.99949	355.99986	1.0
$C_{10}H_{17}NO_5\\$	$[M+I]^-$	358.01514	358.01532	0.5
$C_{10}H_{15}NO_6\\$	[M+I] <sup>-</sup>	371.99441	371.99446	0.1
$C_{10}H_{17}NO_6\\$	[M+I] <sup>-</sup>	374.01006	374.01079	1.9
$C_{10}H_{17}NO_7\\$	[M+I] <sup>-</sup>	390.00497	390.97405	0.1

**Table S4.** Molecular formulas, ions, and mass accuracies of assigned gas-phase products detected by I-CIMS in the reaction of  $\alpha$ -pinene with OH radicals in the presence of NO<sub>x</sub>.

Molecular	Ion	Exact	Observed	Mass
Formula		Mass (Da)	Mass (Da)	Accuracy (ppm)
$C_{10}H_{16}O_2$	$[M+I]^-$	295.01950	295.02105	5.3
$C_{10}H_{16}O_3$	$[M+I]^-$	311.01441	311.01442	4.1
$C_{10}H_{15}NO_4\\$	$[M+I]^-$	340.00458	340.00326	-3.9
$C_{10}H_{17}NO_4\\$	$[M+I]^-$	342.02023	342.02178	4.5
$C_{10}C_{16}O_{5}$	[M+1] <sup>-</sup>	343.00479	343.00699	6.4
$C_{10}H_{15}NO_5\\$	$[M+I]^-$	355.99949	356.00111	4.5
$C_{10}H_{17}NO_5\\$	$[M+I]^-$	358.01514	358.01683	4.7
$C_9H_{15}NO_6$	$[M+I]^-$	359.99441	359.99532	2.5
$C_{10}H_{15}NO_{6}$	[M+I]-	371.99441	371.99628	5.0

**Table S5.** Molecular formulas, ions, and mass accuracies of assigned gas-phase products detected by I-CIMS in the reaction of limonene with OH radicals in the presence of  $NO_x$ .

Molecular Formula	Ion	Exact Mass (Da)	Observed Mass (Da)	Mass Accuracy (ppm)
C <sub>4</sub> H <sub>7</sub> NO <sub>5</sub>	[M+I]-	275.9374	275.9371	-1.1
$C_6H_{11}NO_5$	[M+I]-	303.9687	303.9678	-3.0
$C_{10}H_{16}O_2$	[M+I]-	295.01950	295.01995	1.5
$C_{10}H_{17}NO_4\\$	[M+I]-	342.02023	342.02069	1.4
$C_{10}H_{15}NO_{5}$	[M+I]-	355.99949	355.99997	1.3
$C_{10}H_{17}NO_5\\$	[M+I]-	358.01514	358.01555	1.1
$C_{10}H_{15}NO_6 \\$	[M+I]-	371.99441	371.99483	1.1
C <sub>10</sub> H <sub>15</sub> NO <sub>7</sub>	[M+I]-	387.98932	387.98984	1.3

**Table S6.** Molecular formulas, ions, and mass accuracies of assigned gas-phase products detected by I-CIMS in the reactions of ocimene with OH radicals in the presence of NO<sub>x</sub>.

Molecular Formula	Ion	Exact Mass (Da)	Observed Mass (Da)	Mass Accuracy (ppm)
C <sub>10</sub> H <sub>17</sub> NO <sub>4</sub>	[M+I] <sup>-</sup>	342.02023	342.02016	-0.2
$C_{10}H_{17}NO_{5}$	[M+I] <sup>-</sup>	358.01514	358.01474	-1.1
$C_{10}H_{17}NO_6$	[M+I] <sup>-</sup>	374.01006	374.00975	-0.8

**Table S7**. Ions and molecular formulas of unassigned products detected by I-CIMS in the reactions of  $\Delta$ -3-carene,  $\beta$ -pinene,  $\alpha$ -pinene, limonene, and ocimene with OH radicals in the presence of  $NO_x$ .

I-CIMS Mass	Molecular Formula	Δ-3-Carene	β-Pinene	α-Pinene	Limonene	Ocimene
269	C <sub>7</sub> H <sub>10</sub> O <sub>3</sub>					X
269	C <sub>8</sub> H <sub>14</sub> O <sub>2</sub>					X
283	C <sub>8</sub> H <sub>12</sub> O <sub>3</sub>			X		
285	C <sub>7</sub> H <sub>10</sub> O <sub>4</sub>			X		
285	C <sub>8</sub> H <sub>14</sub> O <sub>3</sub>			X		
285	C <sub>9</sub> H <sub>18</sub> O <sub>2</sub>			X		
288	C <sub>5</sub> H <sub>7</sub> NO <sub>5</sub>	X				X
288	C <sub>6</sub> H <sub>11</sub> NO <sub>4</sub>					X
297	C <sub>9</sub> H <sub>14</sub> NO <sub>3</sub>		X			
300	C <sub>7</sub> H <sub>11</sub> NO <sub>4</sub>			X		
302	C <sub>6</sub> H <sub>9</sub> NO <sub>5</sub>	X	X			
304	C <sub>5</sub> H <sub>7</sub> NO <sub>6</sub>					X
306	C <sub>6</sub> H <sub>13</sub> NO <sub>5</sub>		X			
314	C7H9NO5		X			
316	C <sub>7</sub> H <sub>11</sub> NO <sub>5</sub>	X	X			
318	C <sub>7</sub> H <sub>13</sub> NO <sub>5</sub>		X			
318	C <sub>6</sub> H <sub>9</sub> NO <sub>6</sub>		X			
320	C <sub>5</sub> H <sub>7</sub> NO <sub>7</sub>	X	X			
320	C <sub>6</sub> H <sub>11</sub> NO <sub>6</sub>		X			X
328	C <sub>9</sub> H <sub>15</sub> NO <sub>4</sub>	X		X		
330	C7H9NO6		X			
330	C <sub>8</sub> H <sub>13</sub> NO <sub>5</sub>	X	X	X		
332	C <sub>7</sub> H <sub>11</sub> NO <sub>6</sub>		X			
332	C <sub>6</sub> H <sub>7</sub> NO <sub>7</sub>		X			
342	C <sub>9</sub> H <sub>13</sub> NO <sub>5</sub>		X			
344	C <sub>9</sub> H <sub>15</sub> NO <sub>5</sub>		X	X	X	
374	C <sub>9</sub> H <sub>13</sub> NO <sub>7</sub>		X			

**Table S8.** Molecular formulas, ions, and mass accuracies of assigned SOA products of the reactions of  $\beta$ -pinene and ocimene with OH radicals in the presence of NO<sub>x</sub> detected by ESI-MS.

Molecular Formula	Ion	Exact Mass (Da)	Observed Mass (Da)	Mass Accuracy (ppm)
$C_{10}H_{18}O_4$	[M+Na] <sup>+</sup>	225.1103	225.1104	0.4
C101118O4	[2M+Na] <sup>+</sup>	427.2308	427.2288	-4.7
$C_{10}H_{17}NO_6 \\$	[M+Na] <sup>+</sup>	270.0954	270.0959	1.9
СНМО-	$[M+Na]^+$	286.0903	286.0890	-4.5
$C_{10}H_{17}NO_{7}$	[2M+Na] <sup>+</sup>	549.1908	549.1894	-2.5